Energy growth in viscous channel flows

By SATISH C. REDDY[1] AND DAN S. HENNINGSON[2]

[1] Courant Institute of Mathematical Sciences, New York University, New York, NY 10012 USA

[2] Department of Mathematics, Massachusetts Institute of Technology, Cambridge, MA 02139 USA *and* Aeronautical Research Institute of Sweden (FFA), Box 11021, S-16111 Bromma, Sweden

In recent work it has been shown that there can be substantial transient growth in the energy of small perturbations to plane Poiseuille and Couette flows if the Reynolds number is below the critical value predicted by linear stability analysis. This growth, which may be as large as $O(1000)$, occurs in the absence of nonlinear effects and can be explained by the non-normality of the governing linear operator – that is, the non-orthogonality of the associated eigenfunctions. In this paper we study various aspects of this energy growth for two- and three-dimensional Poiseuille and Couette flows using energy methods, linear stability analysis, and a direct numerical procedure for computing the transient growth. We examine conditions for no energy growth, the dependence of the growth on the streamwise and spanwise wavenumbers, the time dependence of the growth, and the effects of degenerate eigenvalues. We show that the maximum transient growth behaves like $O(R^2)$, where R is the Reynolds number. We derive conditions for no energy growth by applying the Hille–Yosida theorem to the governing linear operator and show that these conditions yield the same results as those derived by energy methods, which can be applied to perturbations of arbitrary amplitude. These results emphasize the fact that subcritical transition can occur for Poiseuille and Couette flows because the governing linear operator is non-normal.

1. Introduction

Linear stability analysis and energy methods are two standard tools for studying the stability of viscous channel flows. Linear stability analysis involves examining the evolution of small perturbations by linearizing the Navier–Stokes equations and yields the Orr–Sommerfeld (O–S) equation. Stability is then determined by examining the O–S eigenvalues. If there is an eigenvalue in the upper half-plane, then there is an exponentially growing mode and the flow is said to be linearly unstable. This analysis has been carried out using both analytical and numerical techniques (Drazin & Reid 1981). The results show that Poiseuille flow is linearly stable if the Reynolds number R is less than $R_c \approx 5772$ (Orszag 1971) and that Couette flow is linearly stable for all Reynolds numbers (Herron 1991).

Energy methods are based on a variational approach and yield conditions for no energy growth for perturbations of arbitrary amplitude. These methods show that there is no energy growth if the Reynolds number is less than $R_g \approx 49.6$ (Busse 1969; Joseph & Carmi 1969) and $R_g \approx 20.7$ (Joseph 1966) for Poiseuille and Couette flows, respectively.

These results do not agree with experimental studies, which show that Poiseuille and Couette flows may become unstable at Reynolds numbers as low as ≈ 1000 (Patel & Head 1969) and ≈ 360 (Lunbladh & Johansson 1991; Tillmark & Alfredsson 1992),

respectively. In recent years several nonlinear theories, including the secondary instability theory, have been developed, giving better agreement with experiments (Drazin & Reid 1981; Herbert 1988).

Thus, linear stability analysis gives conditions for exponential instability and energy methods give conditions for no energy growth. A shortcoming of these methods is that they do not give information when the Reynolds number satisfies $R_g < R < R_c$. In this intermediate case the energy of a small perturbation decays to zero as $t \to \infty$, but there may be transient energy growth before the decay. For two-dimensional perturbations to Poiseuille flow, transient growth by a factor as large ≈ 50 can occur (Farrell 1988; Reddy, Schmid & Henningson 1993; hereinafter referred to as RSH). This growth occurs in the absence of nonlinear effects and can be explained by the non-orthogonality of the O–S eigenfunctions (Orr 1907). In mathematical terms, growth occurs because the Orr–Sommerfeld operator, which is related to the Orr–Sommerfeld equation, is non-normal. For three-dimensional perturbations, growth by a factor $O(1000)$ can occur (Gustavsson 1991; Butler & Farrell 1992).

The purpose of this paper is to investigate various aspects of this transient energy growth, often called algebraic growth. Consider a mean flow with velocity $U(y)$ in the x-direction between infinite plates at $y = \pm 1$. Let $\boldsymbol{u} = (u, v, w)$ be the components of the velocity of a small three-dimensional perturbation and let $\eta = \partial u/\partial z - \partial w/\partial x$ be the y-component of the vorticity. Linearizing the Navier–Stokes equations and eliminating the pressure, we can express the evolution of the perturbation in terms of v and η (Benney & Gustavsson 1981). We have

$$\left(\frac{\partial}{\partial t} + U\frac{\partial}{\partial x}\right)\nabla^2 v - \frac{\mathrm{d}^2 U}{\mathrm{d}y^2}\frac{\partial v}{\partial x} = \frac{1}{R}\nabla^4 v, \quad v(y = \pm 1) = \frac{\partial v}{\partial y}(y = \pm 1) = 0, \tag{1}$$

$$\left(\frac{\partial}{\partial t} + U\frac{\partial}{\partial x}\right)\eta + \frac{\mathrm{d}U}{\mathrm{d}y}\frac{\partial v}{\partial z} = \frac{1}{R}\nabla^2\eta, \quad \eta(y = \pm 1) = 0, \tag{2}$$

with initial conditions. Here ∇^2 denotes the Laplacian and R is the Reynolds number, defined in terms of the channel half-height and the difference in the velocity between the centreline and the wall.

We simplify these equations by expressing v and η as the superposition of Fourier modes in the x- and z-directions:

$$v(x, y, z, t) = \hat{v}(y, t)\,\mathrm{e}^{\mathrm{i}\alpha x + \mathrm{i}\beta z}, \tag{3}$$

$$\eta(x, y, z, t) = \hat{\eta}(y, t)\,\mathrm{e}^{\mathrm{i}\alpha x + \mathrm{i}\beta z}. \tag{4}$$

Here α and β are positive wavenumbers. Substituting (3) and (4) into (1) and (2), we obtain

$$-(\mathrm{D}^2 - k^2)\frac{\partial\hat{v}}{\partial t} = -(\mathrm{D}^2 - k^2)^2\hat{v}/R + \mathrm{i}\alpha U(\mathrm{D}^2 - k^2)\hat{v} - \mathrm{i}\alpha\mathrm{D}^2 U\hat{v}, \tag{5}$$

$$\frac{\partial\hat{\eta}}{\partial t} = -\mathrm{i}\beta\mathrm{D}U\hat{v} - \mathrm{i}\alpha U\hat{\eta} + (\mathrm{D}^2 - k^2)\hat{\eta}/R, \tag{6}$$

$$\hat{v}(\pm 1, t) = \mathrm{D}\hat{v}(\pm 1, t) = \hat{\eta}(\pm 1, t) = 0, \tag{7}$$

where $\mathrm{D} = \partial/\partial y$ and $k^2 = \alpha^2 + \beta^2$. Writing (5) and (6) in vector form (Henningson & Schmid 1992), we obtain

$$\frac{\partial}{\partial t}\begin{bmatrix}\hat{v}\\\hat{\eta}\end{bmatrix} = -\mathrm{i}\begin{bmatrix}\mathscr{L}_{\mathrm{os}} & 0\\\mathscr{L}_{\mathrm{c}} & \mathscr{L}_{\mathrm{sq}}\end{bmatrix}\begin{bmatrix}\hat{v}\\\hat{\eta}\end{bmatrix}, \tag{8}$$

where
$$\mathscr{L}_{\mathrm{os}} = -(\mathrm{D}^2 - k^2)^{-1}[(\mathrm{D}^2 - k^2)^2/(\mathrm{i}R) - \alpha U(\mathrm{D}^2 - k^2) + \alpha \mathrm{D}^2 U], \tag{9}$$

$$\mathscr{L}_{\mathrm{c}} = \beta \mathrm{D} U, \tag{10}$$

$$\mathscr{L}_{\mathrm{sq}} = \alpha U - (\mathrm{D}^2 - k^2)/\mathrm{i}R. \tag{11}$$

The operators $\mathscr{L}_{\mathrm{os}}$ and $\mathscr{L}_{\mathrm{sq}}$ are called the Orr–Sommerfeld and Squire (Sq) operators, respectively. We call $\mathscr{L}_{\mathrm{c}}$ the coupling operator and let $\mathscr{L}$ denote the full block matrix in (8). The evolution of a two-dimensional perturbation is determined by the operator $\mathscr{L}_{\mathrm{os}}$. For three-dimensional perturbations, $\beta \neq 0$, and the normal vorticity is forced by the velocity.

We can write the solution to (8) in terms of an eigenfunction expansion, since the eigenfunctions form a complete set (Diprima & Habetler 1969; Herron 1980). Let $\{\lambda_j\}$ and $\{\mu_j\}$ denote the eigenvalues of $\mathscr{L}_{\mathrm{os}}$ and $\mathscr{L}_{\mathrm{sq}}$, respectively. If the eigenvalues are distinct, then

$$\hat{v}(y, t) = \begin{bmatrix} \hat{v}(y, t) \\ \hat{\eta}(y, t) \end{bmatrix} = \sum_j A_j \exp(-\mathrm{i}\lambda_j t) \begin{bmatrix} \tilde{v}_j(y) \\ \tilde{\eta}_j^p(y) \end{bmatrix} + \sum_j B_j \exp(-\mathrm{i}\mu_j t) \begin{bmatrix} 0 \\ \tilde{\eta}_j(y) \end{bmatrix}. \tag{12}$$

The vector eigenfunctions in the first sum are called the O–S modes; the functions $\{\tilde{v}_j\}$ are the eigenfunctions of $\mathscr{L}_{\mathrm{os}}$, and the functions $\{\tilde{\eta}_j^p\}$ are the forced normal vorticity functions corresponding to the velocity functions. The vector eigenfunctions in the second sum are the Sq modes, and the functions $\{\tilde{\eta}_j\}$ are the eigenfunctions of $\mathscr{L}_{\mathrm{sq}}$. The coefficients $\{A_j\}$ and $\{B_j\}$ depend on the initial condition $\hat{v}(y, 0)$.

A physically relevant quantity for measuring growth is the energy norm:

$$\|\hat{v}\|^2 = \int_{-1}^{1} (|\mathrm{D}\hat{v}|^2 + k^2|\hat{v}|^2 + |\hat{\eta}|^2) \, \mathrm{d}y. \tag{13}$$

The quantity $\|\hat{v}\|^2$ is proportional to the energy of the perturbation $\hat{v}$. The total energy of the perturbation $\boldsymbol{u}$ is obtained by first dividing $\|\hat{v}\|^2$ by $2k^2$ and then integrating the resulting quantity over all α and β (Gustavsson 1986). The growth function

$$G(\alpha, \beta, R, t) \equiv G(t) = \sup_{\hat{v}(\cdot, 0) \neq 0} \frac{\|\hat{v}(\cdot, t)\|^2}{\|\hat{v}(\cdot, 0)\|^2}, \tag{14}$$

measures the greatest possible growth in energy of an initial perturbation at time t. We denote the maximum growth for all time as $G^{\max}(\alpha, \beta, R) \equiv G^{\max} = \sup_{t \geqslant 0} G(t)$. By definition $G^{\max} \geqslant 1$. There is no energy growth if $G^{\max} = 1$.

There has been much work on algebraic growth in viscous channel flows at subcritical Reynolds numbers. The focus of much of the early work was on degeneracies of the O–S eigenvalues and exact resonances between the O–S and Sq eigenvalues as possible mechanisms for growth (Gustavsson & Hultgren 1980; Gustavsson 1986; Shantini 1989). (An exact resonance occurs if an O–S eigenvalue λ_j and a Sq eigenvalue μ_k coincide.) The motivation for this approach is that if there is a degeneracy or exact resonance, then the solution (12) will have additional terms of the form $t \exp(-\mathrm{i}\lambda_j t)$, suggesting the possibility of algebraic growth even if $\mathrm{Im}\,\lambda_j < 0$. Various results on degeneracies and resonances for Couette and Poiseuille flows were obtained, but significant energy growth was not found.

Degeneracies and resonances are not required for growth. Energy growth can occur if the operator $\mathscr{L}$ is non-normal; that is, if it has non-orthogonal eigenfunctions (the inner product implicit in this statement is defined in §2). In general, it may be inappropriate to analyse the behaviour of a non-normal operator using its spectrum alone; see §4 for a description of pseudospectra, an alternative method of analysis (Trefethen 1992). Non-orthogonality can lead to coefficients $\{A_j\}$ and $\{B_j\}$ being much

larger than $\|\hat{v}\|$ – sometimes by a factor as large as $O(10^{10})$ (RSH) (here we assume that the vector eigenfunctions are scaled so that they have norm 1. If the eigenfunctions were orthogonal, then the sum of the squares of the coefficients would equal $\|\hat{v}\|^2$). Suppose that $\hat{v}$ in (12) has energy 1 and is the sum of terms with large coefficients. At $t = 0$, the large terms approximately cancel. However, for moderate $t > 0$, (12) is still a sum of large terms even if all the exponential terms decay. The initial cancellation need not occur, so it is possible for the energy of the perturbation to be larger than its initial value.

In recent work, Henningson (1991) considered the near coincidence of an O–S and Sq eigenvalue, called near resonance, as a possible mechanism for growth for Poiseuille flow. He found that the expansion coefficients of an initial perturbation with zero normal vorticity can be relatively large and that such perturbations can lead to large growth in the amplitude of the normal vorticity. Gustavsson (1991) has investigated this scenario for growth for Poiseuille flow in greater detail. He chose the initial perturbation to have zero normal vorticity and initial velocity equal to the eigenfunction of the O–S operator associated with the least stable mode. He found that the energy in the normal vorticity, the last term in (13), could grow to be $O(1000)$ at subcritical Reynolds numbers. He showed that the maximum growth in the normal vorticity energy for this class of initial perturbation occurs for $\alpha = 0$ and $\beta \approx 2$ when the Reynolds number is fixed. This maximum in the (α, β)-plane is proportional to R^2 and occurs at a time that is proportional to R.

The above procedure gives a lower bound for the growth function since a particular trial initial perturbation is substituted into (14). A direct estimate of the growth function was first performed by Farrell (1988), who investigated growth for two-dimensional perturbations to Poiseuille and Couette flows. His method involves a finite-difference discretization of $\mathscr{L}$ coupled with a variational method. This technique was extended to examine the growth for three-dimensional Poiseuille, Couette, and boundary-layer flows by Butler & Farrell (1992). They show that growth by a factor $O(1000)$ can occur at subcritical Reynolds numbers. Results similar to Gustavsson's are found for the maximum growth G^{max} for Poiseuille flow in the (α, β)-plane. It turns out that the estimated value of G^{max} at $\alpha = 0$ and $\beta = 2$ is only 10% greater than the growth found by Gustavsson. For Couette flow it is found that the maximum energy growth is proportional to R^2 and that growth by a factor $\approx 19\,000$ may occur for $R = 4000$. It is shown that G^{max} is greatest for points slightly off the β-axis. For both flows it is shown that the initial perturbation that achieves the large growth is essentially a streamwise vortex.

The transient growth described above is physically due to the tilting of the mean spanwise vorticity towards the normal direction by the normal velocity. This is represented by the operator $\mathscr{L}_c$. Another interpretation, first put forward by Landahl (1975), is that of lift-up. The generation of normal vorticity can be related to the generation of horizontal disturbance velocities caused by the lift-up of fluid elements in the normal direction such that their horizontal momentum is conserved. These interpretations are discussed by Henningson (1988) and Gustavsson (1991).

The purpose of this paper is to extend the previous work on transient growth at subcritical Reynolds numbers for two- and three-dimensional Couette and Poiseuille flows. We do this by combining an energy method, a direct method for computing growth, and linear stability analysis. Our main goal is to examine the functions $G(\alpha, \beta, R, t)$ and $G^{max}(\alpha, \beta, R)$. In particular, we consider (a) conditions for no energy, (b) dependence of the growth on α and β, (c) the time dependence of the growth, and (d) the effects of degenerate eigenvalues.

We derive conditions for no energy growth by examining the numerical range of $\mathscr{L}$, defined as the union of all numbers of the form $(\mathscr{L}\hat{v}, \hat{v})$, where $\|\hat{v}\|^2 = 1$ and $(\cdot, \cdot)$ is the inner product associated with (13) (Kato 1976). By the Hille–Yosida theorem (Pazy 1983; RSH), there is no energy growth if and only if the numerical range of $\mathscr{L}$ lies in the lower half-plane. For each wavenumber combination, we find that there exists a critical surface $R_1(\alpha, \beta)$ such that there is no energy growth if $R \leqslant R_1(\alpha, \beta)$. We compute the critical surface numerically and also derive asymptotic formulae for it.

Our method for computing transient energy growth is based on the eigenfunction expansion (13) and is similar to the method employed by Butler & Farrell (1992). The main differences are that we use spectral methods to discretize $\mathscr{L}$ and that we attempt to use as few terms in the eigenfunction expansion as possible. These changes substantially reduce the amount of computational work required for the growth calculation, enabling us to examine the parametric dependence of the growth more closely.

Using the numerical procedure, we compute $G^{\mathrm{max}}(\alpha, \beta, R)$ for two- and three-dimensional flows. By extending the approach used by Gustavsson (1991), we show that for small α, $G^{\mathrm{max}}(\alpha, \beta, R)$ effectively depends on $k^2 = \alpha^2 + \beta^2$ and αR. Using this last result, we show that $\sup_{\alpha, \beta} G^{\mathrm{max}}(\alpha, \beta, R) = O(R^2)$ for large subcritical Reynolds numbers for both Poiseuille and Couette flows.

By modifying the eigenfunction expansion (13) to include an algebraic term, we show numerically that $G^{\mathrm{max}}(\alpha, \beta, R)$ is continuous at points in (α, β, R)-space where the O–S operator has a degeneracy or where there is a resonance between an O–S and an Sq eigenvalue.

We also show that the conditions for no growth based on the numerical range of $\mathscr{L}$ are equivalent to those obtained by applying standard energy methods to the full Navier–Stokes equations. This holds because the nonlinear terms in the Navier–Stokes equation drop out of the evolution equation for the energy. We show that this equivalence implies linear transient growth mechanisms are necessary for subcritical transition in Poiseuille and Couette flows.

The paper is organized as follows. Section 2 briefly examines the operators $\mathscr{L}_{\mathrm{sq}}$, $\mathscr{L}_{\mathrm{os}}$, and $\mathscr{L}$. Section 3 describes the method for computing growth. In §4 we define the numerical range and introduce the Hille–Yosida theorem. We also define the ϵ-pseudospectra, a family of sets that can be used to analyse the behaviour of non-normal operators. Section 5 derives conditions for no energy growth. Section 6 summarizes results on the growth function for two-dimensional perturbations in Poiseuille and Couette flow. Section 7 presents results on three-dimensional perturbations. Section 8 presents a discussion of the results.

2. The operators $\mathscr{L}_{\mathrm{sq}}$, $\mathscr{L}_{\mathrm{os}}$ and $\mathscr{L}$

The operator $\mathscr{L}_{\mathrm{sq}}$ is a second-order linear differential operator. Its underlying Hilbert space is $\mathscr{H}_{\mathrm{sq}} = L^2[-1, 1]$. (A Hilbert space is a complete vector space with an inner product.) For $\hat{\eta}_1, \hat{\eta}_2 \in \mathscr{H}_{\mathrm{sq}}$, the inner product is defined by

$$(\hat{\eta}_1, \hat{\eta}_2)_L = \int_{-1}^{1} \hat{\eta}_2^* \hat{\eta}_1 \, \mathrm{d}y. \tag{15}$$

The domain of $\mathscr{L}_{\mathrm{sq}}$, which we denote by $\mathscr{D}(\mathscr{L}_{\mathrm{sq}})$, is the set of functions $\{\phi\}$ having a second derivative in $L^2[-1, 1]$ and satisfying $\phi(\pm 1) = 0$. Using standard results (Kato 1976), it can be shown that the spectrum of $\mathscr{L}_{\mathrm{sq}}$ consists of discrete points in C.

The operator $\mathscr{L}_{os}$ can be written in the form $\mathscr{L}_{os} = \mathscr{B}^{-1}\mathscr{A}$, where

$$\mathscr{A} = (D^2 - k^2)^2/(iR) - \alpha U(D^2 - k^2) + \alpha D^2 U, \tag{16}$$

$$\mathscr{B} = -(D^2 - k^2). \tag{17}$$

This operator was studied in the important paper by DiPrima & Habetler (1969). The underlying Hilbert space $\mathscr{H}_{os}$ is the set of functions $\{\phi\}$ having a second derivative in $L^2[-1, 1]$ and satisfying $\phi(\pm 1) = 0$. For $\hat{v}_1, \hat{v}_2 \in \mathscr{H}_{os}$, the inner product is defined by

$$(\hat{v}_1, \hat{v}_2)_H = (D\hat{v}_1, D\hat{v}_2)_L + k^2(\hat{v}_1, \hat{v}_2)_L. \tag{18}$$

The domain $\mathscr{D}(\mathscr{L}_{os})$ is the set of functions in $\mathscr{H}_{os}$ having a fourth derivative in $L^2[-1, 1]$ and satisfying $\phi(\pm 1) = \phi'(\pm 1) = 0$. The spectrum of $\mathscr{L}_{os}$ consists of discrete points in C and the generalized eigenfunctions of $\mathscr{L}_{os}$ are complete in $\mathscr{H}_{os}$.

The underlying Hilbert space for $\mathscr{L}$ is $\mathscr{H} = \mathscr{H}_{os} \times \mathscr{H}_{sq}$ and its domain is $\mathscr{D}(\mathscr{L}) = \mathscr{D}(\mathscr{L}_{os}) \times \mathscr{D}(\mathscr{L}_{sq})$. The inner product is the sum of (15) and (18). Suppose that $\hat{v}_j = [\hat{v}_j \; \hat{\eta}_j]^T \in \mathscr{H}$ for $j = 1, 2$. The norm in (13) is defined by $\|\hat{v}_1\|^2 = (\hat{v}_1, \hat{v}_1)$, where

$$(\hat{v}_1, \hat{v}_2) = (\hat{v}_1, \hat{v}_2)_H + (\hat{\eta}_1, \hat{\eta}_2)_L. \tag{19}$$

Integrating the first term in (19) by parts and using (17), we can write (19) in the form

$$(\hat{v}_1, \hat{v}_2) = (\mathscr{B}\hat{v}_1, \hat{v}_2)_L + (\hat{\eta}_1, \hat{\eta}_2)_L. \tag{20}$$

3. Procedure for computing the growth

Formally, the solution to (8) is

$$\hat{v}(y, t) = e^{-i\mathscr{L}t}\hat{v}(y, 0). \tag{21}$$

The growth function is then given by

$$G(\alpha, \beta, R, t) = \sup_{\hat{v}(\cdot, 0) \neq 0} \frac{\|\hat{v}(\cdot, t)\|^2}{\|\hat{v}(\cdot, 0)\|^2} = \|e^{-i\mathscr{L}t}\|^2. \tag{22}$$

In this section we show how to approximate the norm in (22).

We begin by first rewriting the solution (9). Let $\{\lambda_j\}$ denote the O–S and Sq eigenvalues arranged in order of decreasing imaginary part and let

$$\tilde{q}_j = \begin{bmatrix} \tilde{v}_j \\ \tilde{\eta}_j \end{bmatrix} \tag{23}$$

denote the vector eigenfunctions associated with λ_j. The set $\{\tilde{q}_j\}$ includes both the O–S and Sq modes. As is well known, the eigenvalues satisfy $\operatorname{Im} \lambda_j \to -\infty$ as $j \to \infty$. Rewriting (12), we have

$$\hat{v}(y, t) = \sum_{j=1}^{\infty} \kappa_j(0) \exp(-i\lambda_j t)\, \tilde{q}_j(y) = \sum_{j=1}^{\infty} \kappa_j(t)\, \tilde{q}_j(y). \tag{24}$$

It is clear that if $\operatorname{Im} \lambda_j \ll 0$ and the coefficients $\{\kappa_j(0)\}$ are of 'moderate' magnitude, then the terms for large j will be negligible for $t > 0$. Hence, for sufficiently large K, we have

$$\hat{v}(y, t) \approx \hat{v}_K(y, t) = \sum_{j=1}^{K} \kappa_j(t)\, \tilde{q}_j(y). \tag{25}$$

We let $W \equiv W_K$ denote the space spanned by the first K eigenfunctions.

For each $t > 0$ there is an initial perturbation $\hat{v}(y, 0)$, normalized so that

$$\|\hat{v}(\cdot, 0)\| = 1,$$

such that the energy of the perturbation at time t is $G(\alpha, \beta, R, t)$. The approximation (25) suggests that the growth function can be estimated by considering initial conditions in the finite dimensional space W. We therefore define

$$G_K(t) \equiv G_K(\alpha, \beta, R, t) = \sup_{\hat{v}_K(y, 0) \in W} \frac{\|\hat{v}_K(\cdot, t)\|^2}{\|\hat{v}_K(\cdot, 0)\|^2}. \tag{26}$$

We will demonstrate below by an example that $G_K(t) \approx G(t)$ if K is sufficiently large. First, we show how to compute G_K. Let $\kappa(t) = (\kappa_1(t), \kappa_2(t), \ldots, \kappa_K(t))^{\mathrm{T}}$ denote the vector of the expansion coefficients. By (24), we have $\kappa_j(t) = \exp(-i\lambda_j t)\kappa_j(0)$. Writing this in vector form, we have

$$\kappa(t) = \exp(-i\Lambda_K t)\kappa(0), \tag{27}$$

where Λ_K is the matrix of dimension K with the first K eigenvalues $\{\lambda_j\}$ on the diagonal. The matrix exponential $\exp(-i\Lambda_K t)$ has the terms $\exp(-i\lambda_j t)$ on the diagonal. We can compute the energy of the perturbation $\hat{v}_K$ by substituting (25) into (13). We obtain $\|\hat{v}_K\|^2 = \kappa^*(t) A \kappa(t)$, where A is the matrix defined in terms of the inner product (19):

$$A_{jl} = (\tilde{q}_j, \tilde{q}_l). \tag{28}$$

The matrix A is Hermitian and can be decomposed in the form $A = F^*F$, where F^* is the Hermitian conjugate of F. It follows that

$$\|\hat{v}_K(t)\|^2 = \kappa^*(t) F^*F\kappa(t) = \|F\kappa(t)\|_2^2, \tag{29}$$

where the subscript 2 denotes the 2-norm (Euclidian norm). The procedure for determining $G_K(t)$ now follows that outlined in RSH. We have

$$G_K(t) = \sup_{\kappa(0) \neq 0} \frac{\|F\kappa(t)\|_2^2}{\|F\kappa(0)\|_2^2} = \sup_{\kappa(0) \neq 0} \frac{\|F\exp(-i\Lambda_K t)\kappa(0)\|_2^2}{\|F\kappa(0)\|_2^2} = \|F\exp(-i\Lambda_K t)F^{-1}\|_2^2. \tag{30}$$

The crucial feature of this last formula is that the 2-norm of any matrix can be determined using the singular value decomposition (SVD), which can be computed using *standard subroutines available in most software libraries*. The SVD yields both $G_K(t)$ and the coefficients $\{\kappa(0)\}$ of the initial condition that achieve this supremum. Hence, to compute the growth function $G_K(t)$ we only need the eigenvalues $\{\lambda_j\}$ and the vector eigenfunctions $\{\tilde{q}_j\}$. The formula (30) is similar to that employed by Butler & Farrell (1992).

We use a spectral discretization of $\mathscr{L}$ to compute its eigenvalues and eigenfunctions numerically (Herbert 1977; RSH). This procedure converts $\mathscr{L}$ into a matrix L of dimension $\approx 2N$, where N is the degree of the polynomial approximation or the number of modes. (For two-dimensional calculations the dimension of the matrix is $\approx N$.) The amount of work required to compute the eigenvalues and eigenfunctions is $O(N^3)$ arithmetic operations. In the case of Poiseuille flow we exploit the symmetry properties and separately consider the even part of $\mathscr{L}$, corresponding to even velocity and odd vorticity, and the odd part, corresponding to odd velocity and even vorticity. Because we restrict attention to the K least stable modes instead of all $2N$ modes, only $O(K^3)$ (instead of $O(N^3)$) operations are required for the computation in (30). This and the use of spectral methods are the differences between our procedure and that described in Farrell (1988) and Butler & Farrell (1992). These changes can lead to a substantial reduction in the number of arithmetic operations required *to compute the*
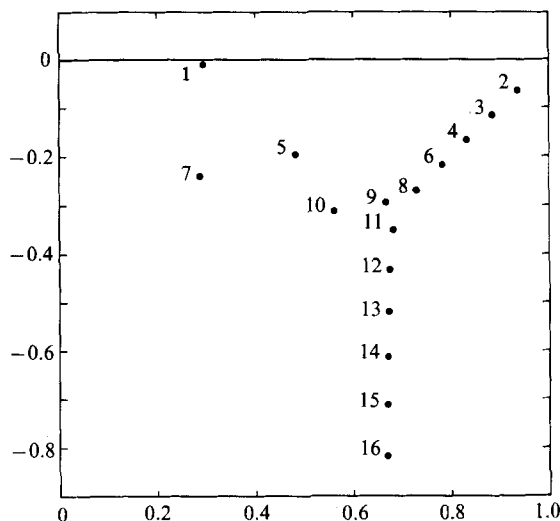
FIGURE 1. Eigenvalues of $\mathscr{L}_{\mathrm{os}}$ for $\alpha = 1$, $\beta = 0$ and $R = 3000$, numbered in order of decreasing imaginary part.
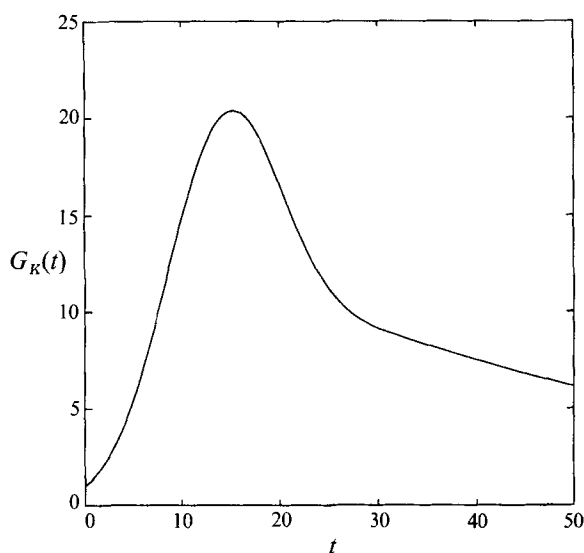

FIGURE 2. Plot of growth function $G_K(\alpha, 0, R, t)$ for $\alpha = 1$, $R = 3000$ and $K = 30$.

growth for two reasons. First, spectral methods can yield accurate approximations of the eigenfunctions and eigenvalues with a smaller N than that required for finite-difference methods. Secondly, K is often much less than $2N$. A reduction in the work by a factor of 5 or more is typical.

The following example illustrates this procedure. We examine two-dimensional Poiseuille flow with $\alpha = 1$ and $R = 3000$ and consider the even part of the O–S operator only. In this case $\mathscr{L} \equiv \mathscr{L}_{\mathrm{os}}$. The ordered eigenvalues of $\mathscr{L}_{\mathrm{os}}$ are shown in figure 1. As $j \to \infty$, we have $\mathrm{Im}\,\lambda_j \to -\infty$ and $\mathrm{Re}\,\lambda_j \approx \frac{2}{3}$.

We start with a computation with $N = 64$ and $K = 30$. Figure 2 plots the growth function $G_K(\alpha, 0, R, t)$. There is significant energy growth ($G_K^{\mathrm{max}} = 20.37$) even though all the eigenvalues lie in the lower half-plane. After the initial transient, the behaviour
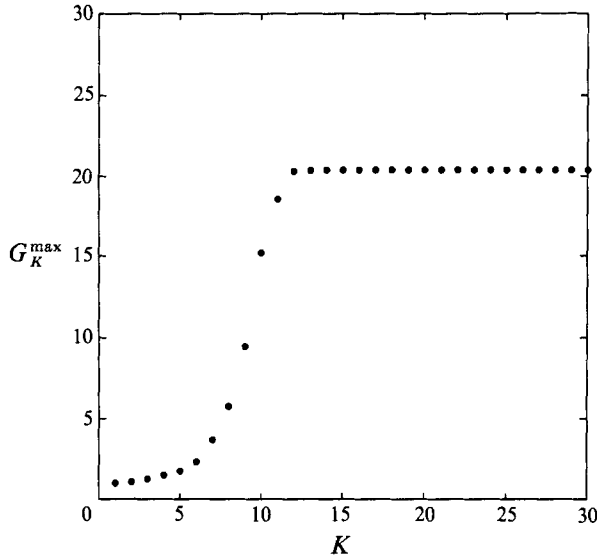
FIGURE 3. Maximum growth $G_K^{\max}(\alpha, 0, R)$ for $\alpha = 1$ and $R = 3000$.
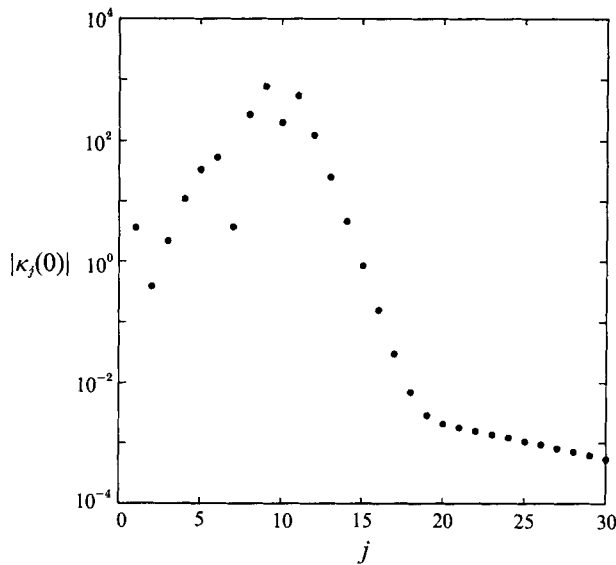

FIGURE 4. Magnitude of the expansion coefficients $\kappa_j(0)$ for the initial velocity perturbation which achieves the maximum growth for $\alpha = 1$ and $R = 3000$.

of the growth function is governed by the eigenvalues near the real axis. Figure 3 shows that $G_K^{\max}$ is essentially independent of K if K is sufficiently large. Also, we find that $G^{\max}$ changes by less than 1% if N is changed to 80 or 96.

In general, to get a good approximation to the growth, K must be sufficiently large so that the modes at the intersection of the three eigenvalue branches are taken into account. The reason is that the associated eigenfunctions are nearly linearly dependent, which implies that the expansion coefficients $\{\kappa_j(0)\}$ of an arbitrary perturbation with unit energy can be large. This is shown in figure 4, where we plot the magnitudes of the expansion coefficients of the normalized initial velocity perturbation which achieves

the maximum growth G^{max}. The largest coefficients correspond to the eigenvalues at the intersection of the branches. The contribution from the modes below the intersection decreases rapidly as j increases. Although it is not reflected in the magnitude of the coefficients, the contribution of the least stable modes is important as well. For example, the maximum growth for an initial condition in the space spanned by $\{\tilde{q}_j\}$ for $j = 2, 3, \ldots, 30$ is only ≈ 6.

For $\alpha \ll 1$ we find that a good approximation to G^{max} can be obtained if all the modes with imaginary part greater than ≈ -2 are included in the growth calculation. For $\alpha = O(1)$, it is sufficient to include the modes with imaginary part greater than $\approx -\alpha$. We have checked that a sufficient number of modes have been retained for the computations presented in this paper so we will drop the subscript K. Our results for Poiseuille and Couette flow agree with the results listed in Butler & Farrell (1992). The principal limitation of the method is that the results may not be accurate when αR is large because it is difficult to compute the eigenvalues and eigenfunctions. We will discuss this in more detail in the next section.

Our numerical computations were performed in double precision on a Sparc 2 workstation using the interactive linear algebra package Matlab.

4. Pseudospectra, the numerical range, and applications to energy growth

An alternative to eigenvalues for analysing the behaviour of non-normal operators is to consider their pseudospectra and numerical range. Let A be a matrix with eigenvalues $\Lambda(A)$ and resolvent set $\rho(A) = C \backslash \Lambda(A)$. The resolvent $(zI - A)^{-1}$ is defined if $z \in \rho(A)$. Let $\|\cdot\|$ denote the norm induced by the inner product $(\cdot, \cdot)$. Here is the definition of pseudospectra (Trefethen 1992):

DEFINITION. *A number $z \in C$ lies in the ϵ-pseudospectrum of A, which we denote by $\Lambda_\epsilon(A)$, if either of the following equivalent conditions is satisfied:*
   (i) *z is an eigenvalue of $A + E$ for some perturbation matrix E with $\|E\| \leqslant \epsilon$;*
   (ii) *$z \in \rho(A)$ and $\|(zI - A)^{-1}\| \geqslant \epsilon^{-1}$ or $z \in \Lambda(A)$.*

The ϵ-pseudospectra are nested sets and $\Lambda_0(A)$ is the spectrum. The definition extends to differential operators. Let $\mathscr{H}$ be a Hilbert space and let $\mathscr{A}: \mathscr{H} \to \mathscr{H}$ be a closed operator with domain $\mathscr{D}(\mathscr{A}) \in \mathscr{H}$. (See Kato (1976) for the definition of a closed operator. The definition of the space $\mathscr{H}$ in §2 ensures that $\mathscr{L}$ is closed.) We take (ii) to be the fundamental definition of the pseudospectrum for operators. Conditions (i) and (ii) are not equivalent for operators but can be made equivalent by taking the closure of (ii).

Here is the definition of the numerical range (Kato 1976):

DEFINITION. *Let A be a linear operator. The numerical range of A, which we denote by $\mathscr{F}(A)$, is defined by*

$$\mathscr{F}(A) = \{z: z = (Au, u), \quad \text{where} \quad u \in \mathscr{D}(A), \|u\| = 1\}. \tag{31}$$

The numerical range is a convex set. For a general class of operators, which includes $\mathscr{L}$, the closure of the numerical range contains the spectrum. (A technical assumption, which is trivially satisfied by $\mathscr{L}_{os}$, $\mathscr{L}_{sq}$ and $\mathscr{L}$, is required for this last result (Kato 1976; RSH).)

In RSH the pseudospectra and the numerical range of the Orr–Sommerfeld operator $\mathscr{L}_{os}$ for two-dimensional Poiseuille flow were studied by approximating the operator by a matrix. It was argued that the approximation is good if the number of modes N is sufficient. Figure 5, taken from RSH, shows the boundaries of the numerical range and
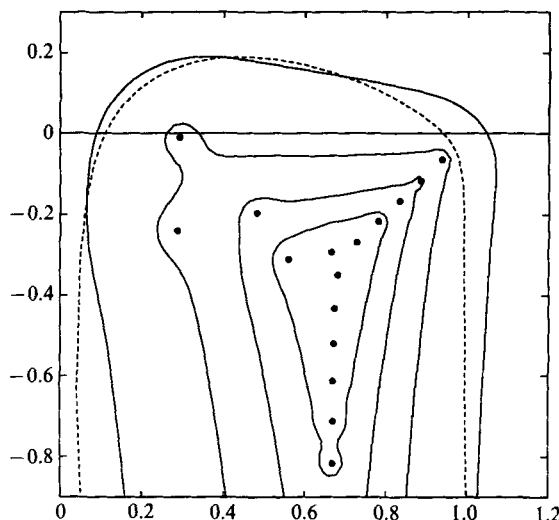
FIGURE 5. Pseudospectra of the even part of the O–S operator $\mathscr{L}_{os}$ for two-dimensional Poiseuille flow with $\alpha = 1$, $\beta = 0$ and $R = 3000$. ●, eigenvalues; – – –, boundary of the numerical range; ——, from outer to inner are boundaries of the ϵ-pseudospectra for $\epsilon = 10^{-1}, 10^{-2}, \ldots, 10^{-4}$.

the ϵ-pseudospectra for the even part of the O–S operator with $\alpha = 1$ and $R = 3000$. (Recall that due to symmetry, even and odd perturbations to Poiseuille flow evolve independently. The even/odd part of the O–S operator governs the evolution of even/odd perturbations.) For each ϵ, the ϵ-pseudospectrum is the region bounded by the contour corresponding to ϵ. As shown in the plot, the sets $\lambda_\epsilon(\mathscr{L}_{os})$ are nested and $\Lambda_0(\mathscr{L}_{os})$ is the spectrum. The dashed line is the boundary of the numerical range.

The main point underlying the study of the ϵ-pseudospectra is that, roughly speaking, operator behaviour depends not solely on the eigenvalues, the points where $\|(zI - A)^{-1}\| \equiv \infty$, but on regions where the resolvent norm $\|(zI - A)^{-1}\|$ is 'large'. For a normal operator the resolvent satisfies (Kato 1976)

$$\|(zI - A)^{-1}\| = \frac{1}{\mathrm{dist}\,\{z, \Lambda(A)\}}, \quad \forall z \notin \Lambda(A), \tag{32}$$

where $\mathrm{dist}\,\{z, \Lambda(A)\}$ is the distance of z to the spectrum. This formula implies that the ϵ-pseudospectrum is simply the union of the closed disks of radius ϵ centred at the eigenvalues. Hence, the ϵ-pseudospectra are not significantly larger than the spectrum if ϵ is small. In many applications, the behaviour of a normal operator is governed by its spectrum. For a non-normal operator, the ϵ-pseudospectrum can be much larger than the spectrum, even if $\epsilon \ll 1$. In such cases it may be more appropriate to consider the pseudospectra instead of the spectrum alone to analyse operator behaviour.

Figure 5 shows that $\mathscr{L}_{os}$ is non-normal. Consider the ϵ-pseudospectrum for $\epsilon = 10^{-4}$, whose boundary is the inner contour. This set is much larger than the union of the disks of radius 10^{-4} centred at the eigenvalues, particularly near the intersection of the eigenvalue branches. These eigenvalues are highly sensitive to perturbations; this property follows from the first characterization of the ϵ-pseudospectrum given in the definition above. This feature of the eigenvalues appears in numerical computations; the eigenvalues at the intersection of the branches cannot be computed to as high a precision as the least stable eigenvalues. Related to the sensitivity is the fact that the associated eigenfunctions are nearly linearly dependent, which implies that eigen-
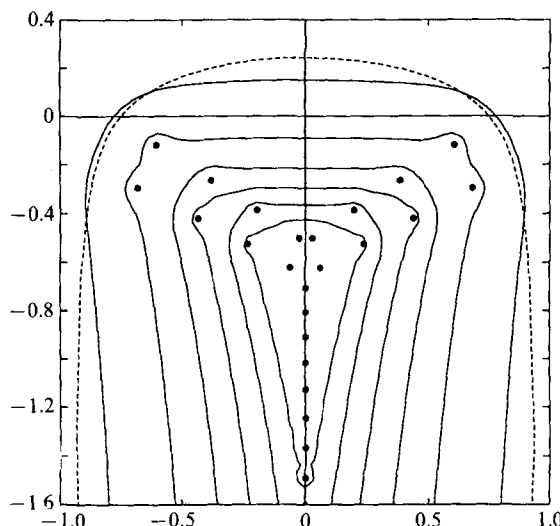
FIGURE 6. Same as figure 5 for the O–S operator $\mathscr{L}_{os}$ for two-dimensional Couette flow with $\alpha = 1$, $\beta = 0$ and $R = 1000$; ——, boundaries of the ϵ-pseudospectra for $\epsilon = 10^{-1}, 10^{-2}, \ldots, 10^{-6}$.

function expansions can involve very large coefficients. These large coefficients can lead to rounding errors as well. In RSH it was shown that both the sensitivity of the eigenvalues and the near linear dependence become dramatically more pronounced as the Reynolds number increases for any fixed α.

Figure 6 plots the boundaries of the numerical range and the ϵ-pseudospectra for two-dimensional Couette flow with $\alpha = 1$ and $R = 1000$. The eigenvalues at the intersection of the branches are highly sensitive to perturbations and the sensitivity again increases dramatically with the Reynolds number.

The pseudospectra and the numerical range of the Sq operator for Couette flow were investigated in RSH. The spectrum also consists of three branches, and it and the ϵ-pseudospectra are symmetric about the imaginary axis. Using analytical methods, it was shown that the numerical range lies in the lower half-plane for all R and that the sensitivity of the eigenvalues at the intersection of the branches increases exponentially as $R \rightarrow \infty$.

The pseudospectra of the full three-dimensional operator $\mathscr{L}$ for both Poiseuille and Couette flow are qualitatively similar to those of the corresponding two-dimensional operator if $\alpha \approx O(1)$. On the other hand, the pseudospectra are different for $\alpha = 0$. Figure 7 shows the pseudospectra for the part of $\mathscr{L}$ governing the evolution of the even velocity and the odd normal vorticity for Poiseuille flow with $\alpha = 0$, $\beta = 2$ and $R = 3000$. The pseudospectra of $\mathscr{L}$ for three-dimensional Couete flow with $\alpha = 0$ is qualitatively similar.

Plots of the pseudospectra of the full Navier–Stokes operator, without fixing α and β, are presented in Trefethen *et al.* (1992).

One of the main applications of pseudospectra and the numerical range is to the analysis of energy growth for initial-value problems like (8) (Pazy 1983). Roughly speaking, energy growth depends on how far the pseudospectra and the numerical range of $\mathscr{L}$ extend into the upper half-plane. Let us define the pseudospectral abscissa to be

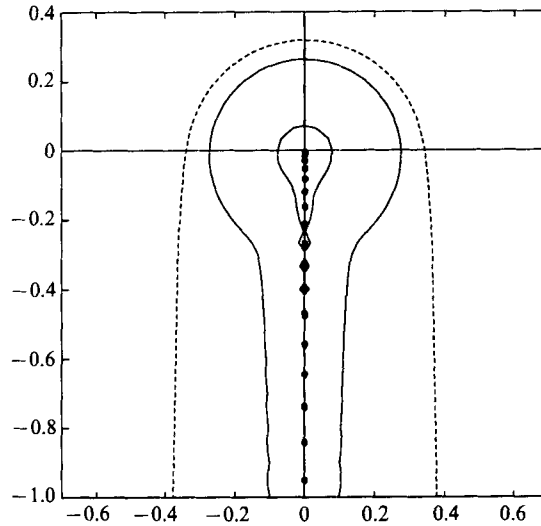$$\gamma_\epsilon = \sup_{z \in \Lambda_\epsilon(\mathscr{L})} \mathrm{Im}\, z, \qquad (33)$$

FIGURE 7. Same as figure 5 for the operator $\mathcal{L}$ for three-dimensional Poiseuille flow with $\alpha = 0$, $\beta = 2$ and $R = 3000$; ———, boundaries of the ϵ-pseudospectra for $\epsilon = 10^{-1}, 10^{-2}$.

and the numerical abscissa to be

$$\omega = \sup_{z \in \mathscr{F}(\mathscr{L})} \operatorname{Im} z. \tag{34}$$

These quantities are simply the maximum imaginary part of any point in the ϵ-pseudospectrum and numerical range, respectively. The following is the main result on energy growth.

THEOREM (HILLE–YOSIDA). *We have* $G^{\max}(\alpha, \beta, R) = 1$ *if and only if any of the following equivalent conditions is satisfied:*

(i) $\gamma_\epsilon \leqslant \epsilon$ *for all* $\epsilon \geqslant 0$;

(ii) $\|(zI - \mathscr{L})^{-1}\| \leqslant 1/(\operatorname{Im} z)$ *for all* z *satisfying* $\operatorname{Im} z > 0$;

(iii) $\omega \leqslant 0$.

Condition (ii) is the standard condition for no energy growth (Pazy 1983), and condition (i) is a restatement of (ii). Condition (iii) states that there is no energy growth if and only if the numerical range of $\mathscr{L}$ lies in the lower half-plane. If $\mathscr{L}$ were normal, the standard condition requiring the eigenvalues $\Lambda(\mathscr{L})$ to lie in the lower half-plane would be necessary and sufficient for no energy growth by the estimate (32) and the condition (ii).

Condition (iii) is related to energy methods (Joseph 1976), which derive conditions for no energy growth by considering the evolution equation for the energy $\|\hat{v}\|^2 = (\hat{v}, \hat{v})$ and can be applied to linear and nonlinear problems. Using (8) and general properties of the inner product, we have

$$\frac{d\|\hat{v}\|^2}{dt} = \left(\hat{v}, \frac{d\hat{v}}{dt}\right) + \left(\frac{d\hat{v}}{dt}, \hat{v}\right) = (\hat{v}, -i\mathscr{L}\hat{v}) + (-i\mathscr{L}\hat{v}, \hat{v}) = 2\operatorname{Im}(\mathscr{L}\hat{v}, \hat{v}). \tag{35}$$

Thus, the rate of change of the energy is always non-positive if and only if the numerical range of $\mathscr{L}$ lies in the lower half-plane.

Condition (iii) can be restated in terms of the anti-symmetric part of $\mathscr{L}$, defined by $\frac{1}{2}(\mathscr{L} - \mathscr{L}^*)$, where $\mathscr{L}^*$ is the adjoint of $\mathscr{L}$. There is no energy growth if and only if the eigenvalues of the anti-symmetric part lie in the lower half-plane; see also Davis (1969) and Galdi & Straughan (1985).

Roughly speaking, the maximum growth $G^{\max}(\alpha, \beta, R)$ depends on how far the pseudospectra extend into the upper half-plane, but the connection is not as precise as in the Hille–Yosida theorem. For each $\epsilon > 0$, let us define $r_\epsilon = \gamma_\epsilon/\epsilon$ and $\tilde{r} = \sup_{\epsilon > 0} r_\epsilon$. We then have (Pazy 1983)

$$G^{\max}(\alpha, \beta, R) \geqslant \tilde{r}^2. \tag{36}$$

An upper bound can be determined using a resolvent integral (Kato 1976).

We can use the Hille–Yosida theorem and (36) to investigate growth in the three examples. In each example, the numerical range extends into the upper half-plane, which implies that there is transient growth. Computing $\tilde{r}$, we find that $G^{\max}$ is at least ≈ 6.3 and ≈ 2.3 for the two-dimensional Poiseuille and Couette problems, respectively. These bounds are approximately one-third of the true value of $G^{\max}$. The bound predicted by (36) for the three-dimensional example is ≈ 850, which is approximately half the actual value of the growth (Trefethen *et al.* 1992).

5. Conditions for no energy growth

We determine conditions for no energy growth by applying the Hille–Yosida theorem. Suppose that $\hat{v} = [\hat{v}\,\hat{\eta}]^{\mathrm{T}} \in \mathscr{H}$. To compute $(\mathscr{L}\hat{v}, \hat{v})$ we note that

$$\mathscr{L}\hat{v} = [\mathscr{L}_{\mathrm{os}}\hat{v} \; \mathscr{L}_{\mathrm{c}}\hat{v} + \mathscr{L}_{\mathrm{sq}}\hat{\eta}]^{\mathrm{T}}.$$

This result and the formula for the inner product (20) imply

$$(\mathscr{L}\hat{v}, \hat{v}) = (\mathscr{A}\hat{v}, \hat{v})_L + (\mathscr{L}_{\mathrm{c}}\hat{v}, \hat{\eta})_L + (\mathscr{L}_{\mathrm{sq}}\hat{\eta}, \hat{\eta})_L. \tag{37}$$

A straightforward calculation shows that

$$\mathrm{Im}\,(\mathscr{L}\hat{v}, \hat{v}) = -\frac{1}{R} \int_{-1}^{1} (|\hat{v}''|^2 + 2k^2|\hat{v}'|^2 + k^4|\hat{v}|^2 + |\hat{\eta}'|^2 + k^2|\hat{\eta}|^2)\,\mathrm{d}y$$

$$+ \mathrm{Im} \int_{-1}^{1} U'(\alpha\hat{v}^*\hat{v}' - \beta\hat{v}^*\hat{\eta})\,\mathrm{d}y, \quad (38)$$

where $'$ denotes the differentiation.

The first term in (38) is strictly negative for all Reynolds numbers and corresponds to dissipation in the energy of the perturbation. The second term may be positive or negative and is related to the exchange of energy with the laminar flow U.

There is no energy growth if $\mathrm{Im}\,(\mathscr{L}\hat{v}, \hat{v}) \leqslant 0$ for all vector functions $\hat{v} \in \mathscr{D}(\mathscr{L})$. The second term (38) is bounded in magnitude. Hence, if the Reynolds number is sufficiently small, then the numerical range will lie in the lower half-plane. Now, if $R_1(\alpha, \beta)$ is the largest value of R such that the numerical range lies in the lower half-plane, then

$$\frac{1}{R_1(\alpha, \beta)} = \sup_{\hat{v} \in \mathscr{D}(\mathscr{L})} \frac{\mathrm{Im} \int (\alpha U'\hat{v}^*\hat{v}' - \beta U'\hat{v}^*\hat{\eta})\,\mathrm{d}y}{\int (|\hat{v}''|^2 + 2k^2|\hat{v}'|^2 + k^4|\hat{v}|^2 + |\hat{\eta}'|^2 + k^2|\hat{\eta}|^2)\,\mathrm{d}y}. \tag{39}$$

This optimization problem can be solved using calculus of variations. The Euler equation corresponding to (39) is the coupled eigenvalue problem

$$\hat{v}^{(iv)} - 2k^2\hat{v}'' + k^4\hat{v} + i\lambda(\alpha U'\hat{v}' + \tfrac{1}{2}\alpha U''\hat{v} - \tfrac{1}{2}\beta U'\hat{\eta}) = 0, \tag{40}$$

$$-\hat{\eta}'' + k^2\hat{\eta} - i\lambda\tfrac{1}{2}\beta U'\hat{v} = 0, \tag{41}$$

$$\hat{v}(\pm 1) = \hat{v}'(\pm 1) = \hat{\eta}(\pm 1) = 0. \tag{42}$$

The function $R_1(\alpha, \beta)$ is the smallest positive eigenvalue λ of (40)–(42). Now, if $\beta = 0$, then (41) is not required, and $R_1(\alpha, 0)$ is the smallest positive eigenvalue of

$$\hat{v}^{(iv)} - 2k^2\hat{v}'' + k^4\hat{v} + i\alpha\lambda(U'\hat{v}' + \tfrac{1}{2}U''\hat{v}) = 0 \quad \hat{v}(\pm 1) = \hat{v}'(\pm 1) = 0. \tag{43}$$

This last eigenvalue problem was first derived by Orr (1907) using energy methods and was subsequently derived by Synge (1938) using a procedure similar to that above. We compute $R_1(\alpha, \beta)$ using a spectral collocation method (Canuto *et al.* 1988).

The expression (38) gives the rate of change of energy of the perturbation $\hat{v}$ for the wavenumber (α, β). The rate of change of the total perturbation energy $\mathscr{E}$ of a perturbation $\boldsymbol{u} = (u, v, w)$ of arbitrary amplitude is given by the Reynolds–Orr equation (Drazin & Reid 1981). We have

$$\frac{d\mathscr{E}}{dt} = -\frac{1}{R}\int (|\nabla u|^2 + |\nabla v|^2 + |\nabla w|^2)\,dx - \int U'(y)\,uv\,dx, \tag{44}$$

where the integration is over the volume between the plates at $y = \pm 1$ and $U \equiv U(y)$ is again the flow in the x-direction. The right-hand side of (44) is analogous to (38).

Equation (44) is the starting point for energy methods. The Reynolds number R_g, below which there is no energy growth, is given by

$$\frac{1}{R_g} = \sup_{\boldsymbol{u}} \frac{-\displaystyle\int U'(y)\,uv\,dx}{\displaystyle\int (|\nabla u|^2 + |\nabla v|^2 + |\nabla w|^2)\,dx}, \tag{45}$$

where $\boldsymbol{u}$ is an admissible perturbation satisfying the continuity equation and the no-slip boundary conditions on the plates.

Now, (38) can be derived from (44). Let $u = \mathrm{Re}\,\{\hat{u}(y)\,e^{i\alpha x + i\beta z}\}$ and let us similarly define v, w and η. As in Drazin & Reid (1981), where (43) is derived from (44), we proceed by integrating and averaging over one period in the x- and z-directions. For the energy exchange term we obtain

$$-\frac{\alpha\beta}{4\pi^2}\int_{-1}^{1} dy \int_{0}^{2\pi/\alpha} dx \int_{0}^{2\pi/\beta} dz\, U'uv = \frac{1}{2k^2}\,\mathrm{Im}\int_{-1}^{1} dy\, U'\left(\alpha\hat{v}^*\,\hat{v}' - \beta\hat{v}^*\hat{\eta}\right). \tag{46}$$

Modulo the factor $2k^2$ in the denominator, which is constant for any fixed wavenumber combination, the right-hand side of (46) is the same as the second term in (38). Using the same procedure, it can be shown that the first term in (44) is the same as the dissipation term in (38), except for a factor of $2k^2$.

The above analysis shows that (38), which is based on the linear operator $\mathscr{L}$ and the numerical range, is equivalent to (44), which gives the rate of change of the total energy for a perturbation of arbitrary amplitude. The equality occurs because the nonlinear term $\boldsymbol{u} \cdot \nabla\boldsymbol{u}$ in the Navier–Stokes equation drops out of (44). The standard procedure

for determining R_{g} is to first derive the Euler equations for (45) and then Fourier transform u, v and w (Joseph 1976). It can be shown that the resulting eigenvalue problem is equivalent to (40)–(42). A similar result was proved by Davis (1969) for a convection problem with surface tension and by Galdi & Straughan (1985) for a general class of problems.

The above arguments imply

$$R_{\mathrm{g}} = \inf_{\alpha,\,\beta} R_1(\alpha, \beta). \tag{47}$$

This equality has two interesting implications. First, for there to be a potential for energy growth for the full nonlinear problem, there must be a potential for energy growth for the linear problem. Hence, a linear growth mechanism is required for transition. Secondly, suppose that $\mathscr{L}$ were normal for all α, β, R. In such a case, $R_{\mathrm{c}} \equiv \inf_{\alpha,\,\beta} R_1(\alpha, \beta)$ by (32) and the Hille–Yosida theorem. Coupled with (47), this would imply that there could be no transition at subcritical Reynolds numbers. This implies that subcritical transition occurs for Poiseuille and Couette flows because $\mathscr{L}$ is non-normal.

6. Growth for two-dimensional Poiseuille and Couette flow

6.1. *Growth contours*

We begin by examining the growth function for two-dimensional flows, where $\beta = 0$. There are three types of behaviour to consider for Poiseuille flow. If the Reynolds number is less than $R_1(\alpha, 0)$, the limit predicted by the numerical range, then $G^{\mathrm{max}}(\alpha, 0, R) = 1$. On the other hand, if $\mathscr{L}_{\mathrm{os}}$ has an eigenvalue in the upper half-plane, then the flow is linearly unstable and $G^{\mathrm{max}}(\alpha, 0, R) = \infty$. Finally, if $R > R_1$ and the flow is linearly stable, then there is transient growth. Figure 8, which originally appeared in RSH and is included here for completeness, indicates these three regions in the (R, α)-plane. We see that there can be transient growth as large as ≈ 51 at subcritical Reynolds numbers. If $\mathscr{L}_{\mathrm{os}}$ were normal for all α and R, then $G^{\mathrm{max}} = 1$ and $G^{\mathrm{max}} = \infty$ would be the only possibilities.

Orr (1907) showed that $\min_\alpha R_1(\alpha, 0) \approx 87.7$. This minimum occurs for $\alpha \approx 2.05$. In addition, it has been shown that $R_1(\alpha, 0) \geqslant c_1/\alpha$ as $\alpha \to 0$ and $R_1(\alpha, 0) \geqslant c_2\alpha^2$ as $\alpha \to \infty$ (Synge 1938; Joseph 1969). It follows that for any fixed Reynolds number R, $G^{\mathrm{max}}(\alpha, 0, R) > 1$ if and only if $\alpha_1(R) < \alpha < \alpha_2(R)$.

It is instructive to compare the growth functions $G(\alpha, 0, R, t)$ for stable and unstable flows. Figure 9 plots the growth function for $\alpha = 1$ and $R = 5000$ and $\alpha = 1$ and $R = 8000$. For small values of t, the growth function is qualitatively the same in the two cases. In this transient phase, the behaviour of the growth function does not depend on the stability or instability of the flow; the stability of the flow is only revealed as $t \to \infty$. The least stable eigenvalues govern the behaviour of the growth function only for large time. The transient growth for stable flows is a short-time phenomenon compared to the infinite growth for unstable flows. The third curve in figure 9 shows the energy of the perturbation velocity $\hat{v}$ in the case where the initial velocity is the normalized eigenfunction associated with the unstable eigenvalue for $\alpha = 1$ and $R = 8000$. The unstable mode does not achieve the greatest possible energy growth; the initial condition which achieves the maximum growth is a linear combination of several eigenfunctions (Farrell 1988).

For Couette flow, there are only two types of behaviour to consider, since the flow is linearly stable for all R. Figure 10 shows the level curves of $G^{\mathrm{max}}(\alpha, 0, R)$. The dashed
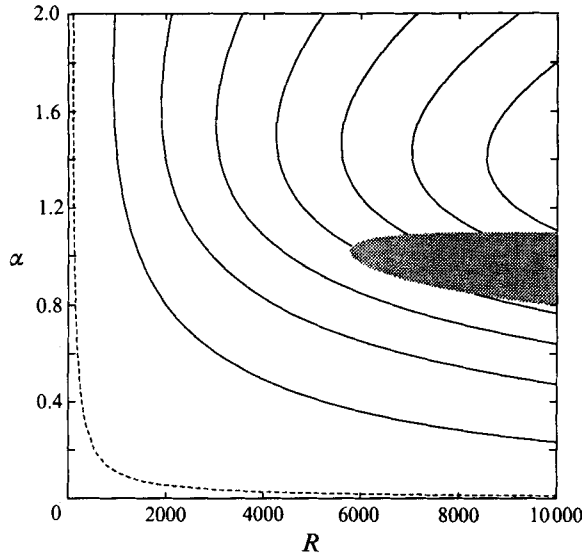
FIGURE 8. Level curves of $G^{max}(\alpha, 0, R)$ for Poiseuille flow. $---$, $G^{max}(\alpha, 0, R) = 1$; ——, from left to right, $G^{max}(\alpha, 0, R) = 10, 20, 30, \ldots, 70$. In the shaded region the flow is linearly unstable.
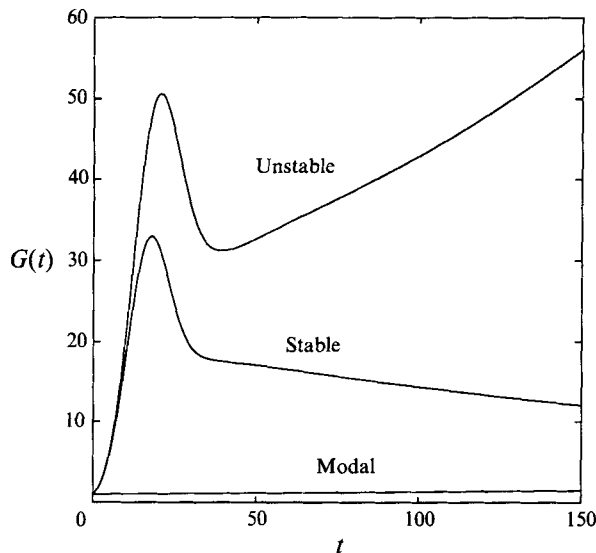

FIGURE 9. Plot of $G(\alpha, 0, R, t)$ for stable and unstable Poiseuille flow. The stable case corresponds to $\alpha = 1$ and $R = 5000$, and the unstable to $\alpha = 1$ and $R = 8000$. The curve labelled 'Modal' is a plot of the perturbation energy in the case where the initial velocity is the normalized eigenfunction corresponding to the unstable eigenvalue for $\alpha = 1$ and $R = 8000$.

line is $R_1(\alpha, 0)$. Orr (1907) showed that $\min_\alpha R_1(\alpha, 0) \approx 44.3$; this occurs for $\alpha \approx 1.88$. The bounds on $R_1(\alpha, 0)$ for the limits $\alpha \to 0$ and $\alpha \to \infty$ given above for Poiseuille flow also hold (with different constants) for Couette flow.

6.2. *Growth at degeneracies in the (R, α)-plane*

Degeneracies of the O–S eigenvalues have received much attention in previous work as a possible mechanism for energy growth. However, degeneracies are neither necessary nor sufficient for growth. It is of fundamental interest to determine the smoothness of
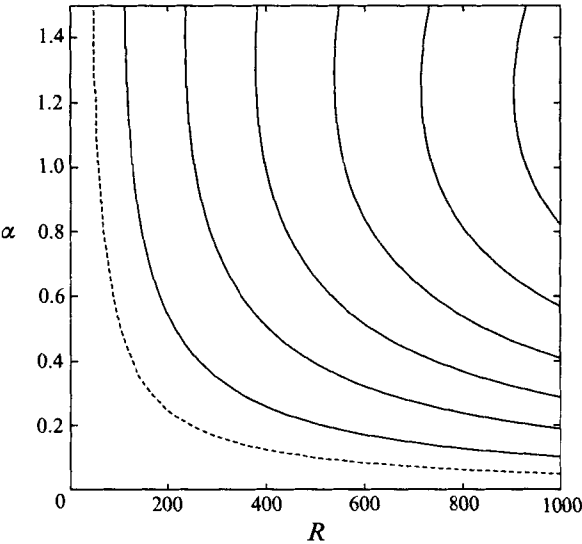
FIGURE 10. Same as figure 8 for Couette flow. The solid curves correspond to $G^{\mathrm{max}} = 2, 4, 6, \ldots, 12$.

R_{d}	α_{d}	$G^{\mathrm{max}}(\alpha_{\mathrm{d}}, 0, R_{\mathrm{d}})$
$8.530\,9600 \times 10^1$	$2.539\,077\,15 \times 10^0$	1.00
$2.790\,0354 \times 10^2$	$1.891\,178\,74 \times 10^0$	2.80
$4.106\,6100 \times 10^2$	$8.858\,196\,00 \times 10^{-1}$	2.35
$1.785\,8440 \times 10^3$	$5.063\,500\,00 \times 10^{-1}$	5.15

TABLE 1. Maximum growth at points where the even part of the O–S operator for Poiseuille flow has a degenerate eigenvalue. The maximum growth is computed to the nearest 0.05. These results were obtained by discretizing $\mathscr{L}_{\mathrm{os}}$ using $N = 64$ even modes.

the maximum growth at the degeneracy points in the (R, α)-plane. To compute the growth the expansion (25) must be modified to include a generalized eigenfunction term; the analysis can be found in many books on ordinary differential equations. If λ_n is a degenerate eigenvalue, then the expansion for the velocity is

$$\hat{v}(y, t) = \kappa_n \tilde{v}_n \exp(-i\lambda_n t) + \partial \kappa_n [\tilde{v}_n t \exp(-i\lambda_n t)$$

$$+ \partial \tilde{v}_n \exp(-i\lambda_n t)] + \sum_{j \neq n}^{K} \kappa_j \tilde{v}_j \exp(-i\lambda_j t). \quad (48)$$

The generalized eigenfunction $\partial \tilde{v}_n$ is determined from the equation $(\mathscr{L}_{\mathrm{os}} - \lambda_n) \partial \tilde{v}_n = i\tilde{v}_n$. Using (48), we can derive a new formula, analogous to (30), for the growth function $G(\alpha, \beta, R, t)$. The principal modification is that the matrix Λ_K now has a non-zero off-diagonal term.

It is conjectured that the O–S operator for Poiseuille flow has degeneracies at an infinite number of discrete points in the (R, α)-plane (Shantini 1989). We examine the maximum growth at the four points in table 1. The criterion for a degeneracy that we used was the existence of a pair of eigenvalues lying within a distance 2×10^{-4} of each other. Because of differences in the numerical procedure, the degeneracies listed in the table differ in the last digits from those listed in Shantini (1989). A check of the eigenfunctions indicates that the points do yield degenerate eigenvalues.
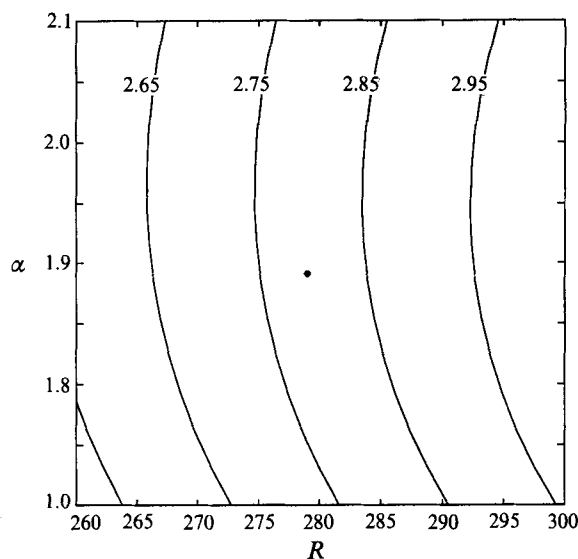
FIGURE 11. Contours of G^{max} for Poiseuille flow in the neighbourhood of the degeneracy at $R \approx 279$ and $\alpha \approx 1.89$ (the dot), where the maximum growth is ≈ 2.80.

R_d	α_d	$G^{max}(\alpha_d, 0, R_d)$
80.565 22	0.5	1.00
114.425 96	0.5	1.05
119.620 36	0.5	1.10
145.797 88	0.5	1.30

TABLE 2. Maximum growth at points where the O–S operator for Couette flow has a degenerate eigenvalue. The maximum growth is computed to the nearest 0.05. These results were obtained by discretizing $\mathcal{L}_{os}$ using $N = 64$ modes.

There is no growth at the first point and this is consistent with figure 8 since the point lies to the left of the $G^{max} = 1$ contour. There is energy growth at the other degeneracies. Figure 11 zooms in on figure 8 in the neighbourhood of the degeneracy near $R \approx 279$ and $\alpha \approx 1.89$. As α and R approach the degeneracy (R_d, α_d), the maximum growth $G^{max}(\alpha, 0, R)$ approaches $G^{max}(\alpha_d, 0, R_d)$; the deviation is at most ± 0.05. Similar results are obtained for the other degeneracies.

The O–S operator for Couette flow has degeneracies at points in the (R, α)-plane as well. In table 2 we list four degeneracies occurring for $\alpha = 0.5$, which we pinpointed with the aid of figures in Gustavsson & Hultgren (1980). Our numerical calculations suggest that $G^{max}(\alpha, 0, R)$ is a smooth function.

7. Growth for three-dimensional Poiseuille and Couette flows

7.1. *The boundary of the region where $G^{max}(\alpha, \beta, R) > 1$*

As discussed in §5, the boundary of the region where $G^{max}(\alpha, \beta, R) > 1$ is defined by the function $R_1(\alpha, \beta)$, the smallest Reynolds number such that there is energy growth for the wavenumber (α, β).

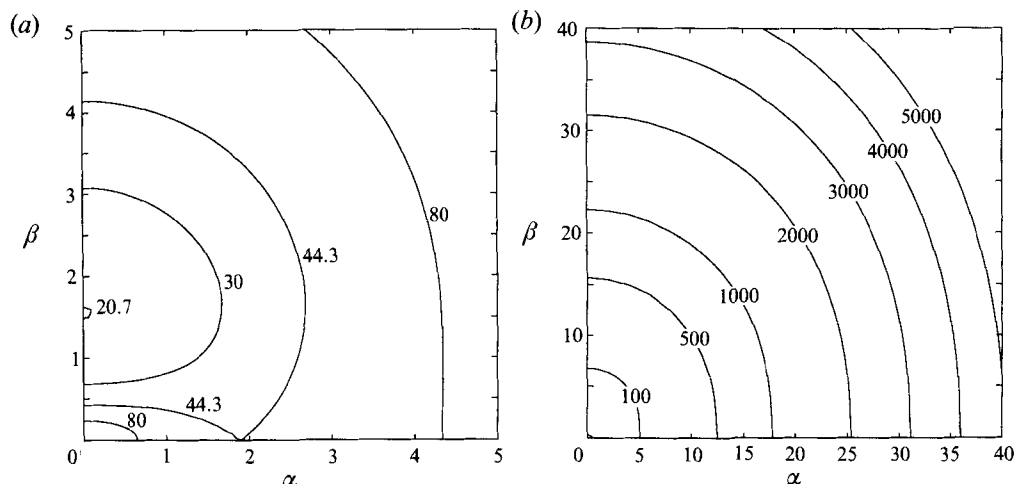Figure 12 shows the level curves of $R_1(\alpha, \beta)$ for Couette flow. For each R, the contour

FIGURE 12. (*a, b*) Level curves of $R_1(\alpha, \beta)$ for Couette flow. The plot (*b*) only shows the outer level curves. The inner curves lie close to the origin.
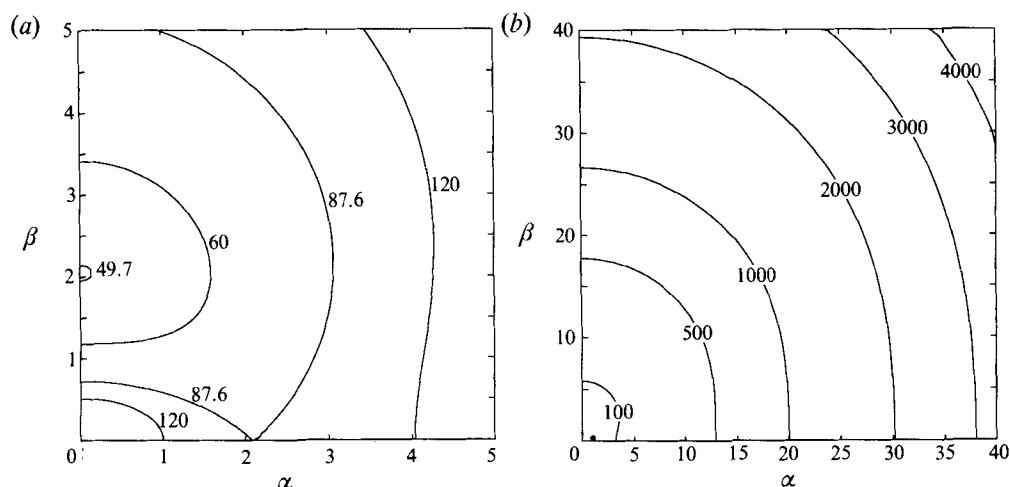

FIGURE 13. (*a, b*) Same as figure 12 for Poiseuille flow. The dot at $\alpha \approx 1$ and $\beta = 0$ in (*b*) roughly marks the region where Poiseuille flow is linearly unstable for $R = 6000$.

$R_1 = R$ is the boundary of the region in the (α, β)-plane where $G^{\max}(\alpha, \beta, R) > 1$. The minimum Reynolds number for energy growth is $R_g = \min R_1(\alpha, \beta) \approx 20.66$, and this value is achieved at $\beta \approx 1.56$ and $\alpha = 0$ (Joseph 1966). Before this last result was obtained, it was thought that Orr's result of ≈ 44.3, which is achieved at $\beta = 0$ and $\alpha \approx 1.88$, gave the minimum Reynolds number for growth. For each $R_1 \geqslant 44.3$ the region where there is energy growth has an annulus-like shape. Figure 12(*b*) shows the outer boundary of the annulus for various values of R_1. Now, $R_1(0, 0) = \infty$ because the operator $\mathscr{L}$ for $\alpha = \beta = 0$ and arbitrary R is normal and has a spectrum lying in the lower half-plane. We show below that $R_1(\alpha, \beta) \to \infty$ as $\alpha, \beta \to 0$.

Figure 13 shows the level curves of $R_1(\alpha, \beta)$ for Poiseuille flow. The minimum Reynolds number in this case is $R_g \approx 49.6$ (Busse 1969; Joseph & Carmi 1969). This is achieved at $\alpha = 0$ and $\beta \approx 2.05$. For each $R > R_c \approx 5772$ there is a small region in the (α, β)-plane for each $R \geqslant R_c \approx 5772$, where the flow is linearly unstable. For

$R = 6000$, this region is approximated by the dot at $\alpha = 1$ and $\beta = 0$ in figure 13(b). The region where there is energy growth is much larger than the region of linear instability.

We can determine analytic bounds for $R_1(\alpha, \beta)$ starting with the expression

$$\mathrm{Im}\,(\mathscr{L}\hat{v}, \hat{v}) = -\frac{1}{R} \int_{-1}^{1} (|\hat{v}''|^2 + 2k^2|\hat{v}'|^2 + k^4|\hat{v}|^2 + |\hat{\eta}'|^2 + k^2|\hat{\eta}|^2)\,\mathrm{d}y$$

$$+ \mathrm{Im} \int_{-1}^{1} U'(\alpha\hat{v}^*\hat{v}'\,\mathrm{d}y - \beta\hat{v}^*\hat{\eta})\,\mathrm{d}y, \quad (49)$$

obtained in §5. We proceed as in (Synge 1938; Joseph 1969). To simplify the notation we define

$$I_j^2 = \int_{-1}^{1} \left|\frac{\mathrm{d}^j\hat{v}}{\mathrm{d}y^j}\right|^2 \mathrm{d}y \quad (j = 0, 1, 2); \quad J_j^2 = \int_{-1}^{1} \left|\frac{\mathrm{d}^j\hat{\eta}}{\mathrm{d}y^j}\right|^2 \mathrm{d}y \quad (j = 0, 1). \quad (50)$$

Dividing (49) by $\|\hat{v}\|^2 = I_1^2 + k^2I_0^2 + J_0^2$ and using the Cauchy–Schwartz inequality, we obtain

$$\omega = \sup_{\lambda \in \mathscr{F}(\mathscr{L})} \mathrm{Im}\,\lambda = \sup_{\hat{v}} \frac{\mathrm{Im}\,(\mathscr{L}\hat{v}, \hat{v})}{\|\hat{v}\|^2} \leqslant \sup_{\hat{v}} \frac{q\alpha I_1 I_0 + q\beta I_0 J_0}{I_1^2 + k^2I_0^2 + J_0^2} - \frac{I_2^2 + 2k^2I_1^2 + k^4I_0^2 + J_1^2 + k^2J_0^2}{R(I_1^2 + k^2I_0^2 + J_0^2)},$$
$$(51)$$

where $q = \sup_{-1 \leqslant y \leqslant 1}|U'(y)|$.

We simplify (51) using the following results, which can be obtained using calculus of variations:

$$I_{j+1}^2 \geqslant \tfrac{1}{4}\pi^2 I_j^2 \quad (j = 0, 1); \qquad J_1^2 \geqslant \tfrac{1}{4}\pi^2 J_0^2. \quad (52)$$

It follows that

$$I_2^2 + 2k^2I_1^2 + k^4I_0^2 + J_1^2 + k^2J_0^2 \geqslant (\tfrac{1}{4}\pi^2 + k^2)(I_1^2 + k^2I_0^2 + J_0^2),$$
$$I_1^2 + k^2I_0^2 \geqslant 2\alpha I_1 I_0,$$
$$k^2I_0^2 + J_0^2 \geqslant 2\beta I_0 J_0.$$

Using these last formulae, we obtain

$$\omega \leqslant q - \frac{\pi^2 + 4k^2}{4R}. \quad (53)$$

Hence, there is no energy growth ($\omega \leqslant 0$) if

$$R \leqslant \frac{\pi^2 + 4k^2}{4q}. \quad (54)$$

The bound (54) is appropriate for large k, but it is not sharp as $k \to \infty$. To obtain a sharp bound for small k we simplify the first term of (51) using the inequality $I_0 \leqslant 2I_1/\pi$. It follows that there is no growth if

$$R \leqslant \frac{\pi(\pi^2 + 4k^2)}{q(2\alpha + 4\beta)}. \quad (55)$$

The inequalities (54) and (55) imply that

$$R_1(\alpha, \beta) \geqslant \max\left\{\frac{\pi^2 + 4k^2}{4q}, \frac{\pi(\pi^2 + 4k^2)}{q(2\alpha + 4\beta)}\right\}. \quad (56)$$

This result shows that the region for growth in the (α, β)-plane lies inside the annulus whose outer and inner boundaries have radii $O(R^{\frac{1}{2}})$ and $O(R^{-1})$ as $R \to \infty$, respectively. For $\beta = 0$, (56) has the same asymptotic form in the limits $\alpha \to 0$ and $\alpha \to \infty$ as the results of Synge and Joseph.
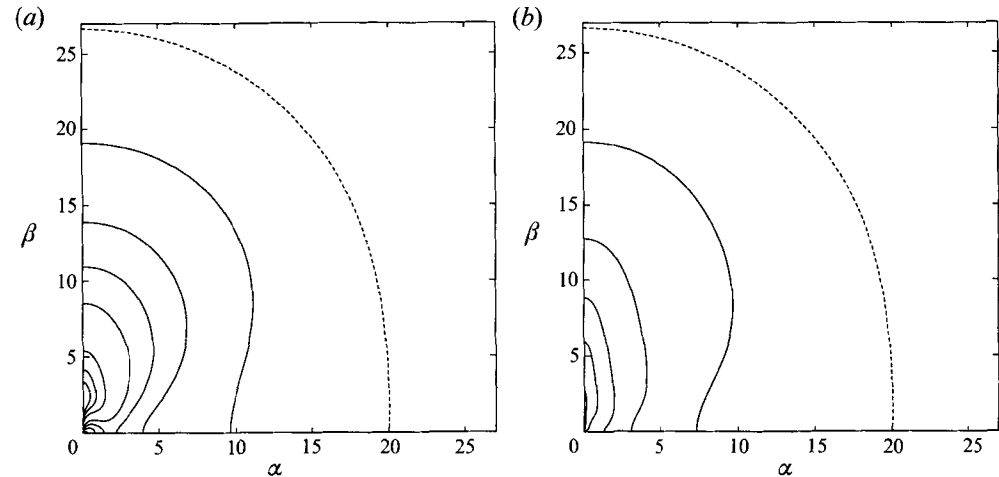
FIGURE 14. (a, b) Contours of G^{max} and t^{max} for Poiseuille flow with $R = 1000$. Plot (a) shows the level curves of G^{max}. ———, $G^{\mathrm{max}} = 1$. ——, from outer to inner, $G^{\mathrm{max}} = 2, 5, 10, 20, 60, 100, 140$. Plot (b) shows the contours of t^{max}. ———, $t^{\mathrm{max}} = 0$. ——, from outer to inner correspond to $t^{\mathrm{max}} = 2, 5, 10, 20, 60$.
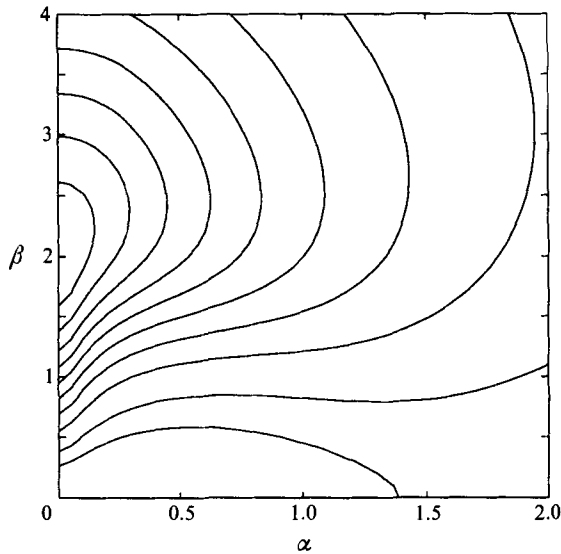

FIGURE 15. Contours of G^{max} for Poiseuille flow with $R = 1000$. The curves from outer to inner correspond to $G^{\mathrm{max}} = 10, 20, 40, \ldots, 140, 160, 180$.

7.2. *Growth contours for Poiseuille flow*

The results of the last section give the boundaries of the region in the (α, β)-plane where there is growth. We now examine various properties of the maximum growth $G^{\mathrm{max}}(\alpha, \beta, R)$ and $t^{\mathrm{max}}(\alpha, \beta, R)$, where t^{max} is the time at which the maximum growth is achieved for Poiseuille flow.

Figure 14 shows the level curves of G^{max} for $R = 1000$ and figure 15 zooms in on the region where G^{max} is largest. Let us define

$$S(R) = \sup_{\alpha, \beta} G^{\mathrm{max}}(\alpha, \beta, R). \tag{57}$$
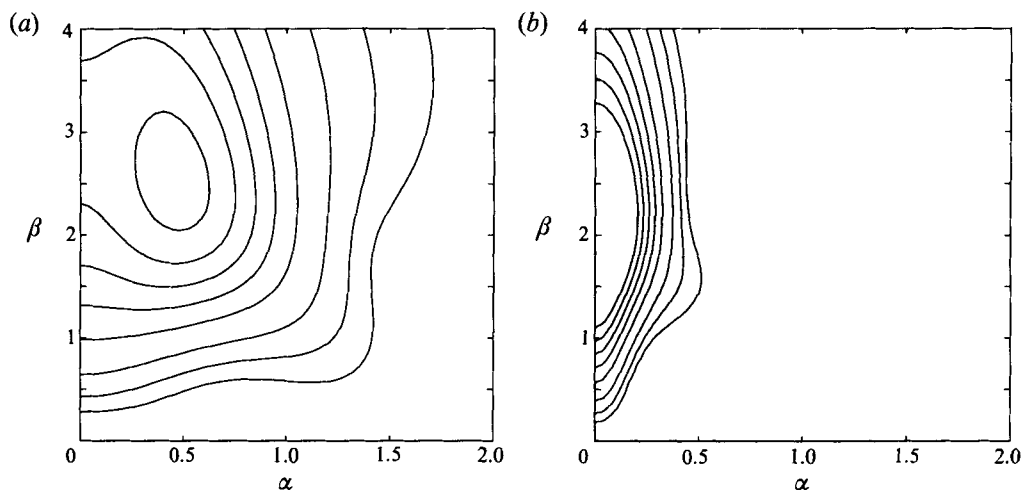
FIGURE 16. (a, b) Level curves of $G(\alpha, \beta, R, t)$, where $t = 25$ in (a) and $t = 75$ in (b). The contours from outer to inner correspond to $G(\alpha, \beta, R, t) = 5, 10, 20, 40, 60, \dots, 120$.

We find that $S(1000) \approx 196$ and that this growth is achieved for $\alpha = 0$ and $\beta \approx 2.05$. In addition, we find that $t^{max}(0, 2.05, 1000) \approx 76$. Note that this wavenumber combination is close to that at which $R_1(\alpha, \beta)$ is minimized. Figure 14(b) shows the level curves of t^{max}. The growth function $G(\alpha, \beta, R, t)$ is maximized at earlier times for wavenumber combinations away from the β-axis. The geometry of the contours of G^{max} and t^{max} is qualitatively similar for different Reynolds numbers and for Couette flow as well.

It is also of interest to consider the behaviour of $G(\alpha, \beta, R, t)$ for fixed t. Figure 16 plots the level curves of the growth function for $t = 25$ and $t = 75$, where the latter time is that at which the global maximum growth of 196 is attained. For $t = 25$ the largest value of $G(\alpha, \beta, R, t)$ occurs away from the β-axis, and the region of large growth is broad. For $t = 75$ the largest value of $G(\alpha, \beta, R, t)$ occurs close to the β-axis and the region of large growth is narrower.

Both $G^{max}(\alpha, \beta, R)$ and $t^{max}(\alpha, \beta, R)$ increase with R for each fixed wavenumber combination. We conjecture that $G^{max}(\alpha, \beta, R) \to \infty$ as $R \to \infty$. This is consistent with the results of Landahl (1980), who showed that the energy of a three-dimensional perturbation to inviscid parallel shear flows may experience unbounded growth. In the next section we will show that $S(R) = O(R^2)$ for large subcritical Reynolds numbers R.

We find that $G^{max}(\alpha, \beta, R)$ is not affected by a direct resonance between the O–S and Sq eigenvalues. For $R = 1000$, there are direct resonances at $\alpha \approx 0.11609$ and $\beta = 1.4731$ and $\alpha \approx 0.22319$ and $\beta = 2.3326$ (Gustavsson 1986). We can determine the growth at these points by including an algebraic term in the eigenfunction expansion, as in the case of degenerate eigenvalues. We find that maximum growth at these points is ≈ 136.5 and ≈ 170, respectively and that $G^{max}(\alpha, \beta, R)$ changes smoothly as α and β are varied. Previously, Butler & Farrell (1992) found that G^{max} is smooth at direct resonances in Couette flow.

It is instructive to further compare the growth for $\alpha = 0$ and $\alpha \neq 0$. Gustavsson (1991) investigates the forcing of the normal vorticity by the least stable O–S mode. In this case the perturbation $\hat{v}$ has a simplified eigenfunction expansion of the form

$$\hat{v}(y, t) = A_1 \exp\left(-i\lambda_1 t\right) \begin{bmatrix} \tilde{v}_1(y) \\ \tilde{\eta}_1^p(y) \end{bmatrix} + \sum_j B_j \exp\left(-i\mu_j t\right) \begin{bmatrix} 0 \\ \tilde{\eta}_j(y) \end{bmatrix}. \tag{58}$$

He chooses the coefficients A_1 and $\{B_j\}$ so that the initial vorticity is zero and $\|\hat{v}\|^2 = 1$. For $\alpha = 0$, $\beta = 1.98$ and $R = 1000$, it is found that there is growth by a factor of ≈ 178 for this choice of perturbation. This growth is only 9% lower than $G^{\max}(0, 1.98, 1000) \approx 196$.

For $\alpha \neq 0$, a perturbation of the form (58) does not yield a good estimate for the maximum growth. For example, for $\alpha = 1$, $\beta = 1.98$, and $R = 1000$, we have $G^{\max} \approx 80$. On the other hand, the maximum growth for a perturbation of the form (58) is only ≈ 7.

The difference between the $\alpha = 0$ and $\alpha = 1$ case is revealed in figure 17, which plots the expansion coefficients for the initial conditions that achieve the maximum energy growths 196 and 80. For $\alpha = 1$, the largest coefficients correspond to the O–S and Sq modes at the intersection of the eigenvalue branches as in the example in §3. Neglecting O–S modes for $j = 2, 3, 4, \ldots$, yields a poor estimate of the growth. For $\alpha = 0$, the largest coefficients in magnitude correspond to the least stable O–S and Sq modes. Hence, the higher O–S modes can be neglected.

In the previous work, Butler & Farrell (1992) investigated growth for Poiseuille and Couette flows. For Poiseuille flow at $R = 5000$, they find that the maximum growth occurs at $\alpha = 0$ and $\beta \approx 2.04$. For Couette flow, they show that $G^{\max}(\alpha, \beta, R)$ is maximized for wavenumber combinations slightly off the β-axis, near $\beta = 1.6$. They note that the potential for growth for small t is greatest away from the β-axis.

7.3. *A scaling for $G^{\max}(\alpha, \beta, R)$*

To get a complete understanding of the behaviour of $G^{\max}(\alpha, \beta, R)$ it is necessary to compute the growth throughout the three-dimensional (α, β, R) parameter space. This approach is computationally expensive. We can get an understanding of the behaviour of $G^{\max}(\alpha, \beta, R)$ for small αR by employing a scaling used by Gustavsson (1991).

Let us define $\bar{t} = t/R$, $\bar{\eta}(y, \bar{t}) = \hat{\eta}(y, t/R)/\beta R$, $\bar{v}(y, \bar{t}) = \hat{v}(y, t/R)$. Then we have $\hat{v}(y, t/R) = [\bar{v}(y, \bar{t}) \, \beta R \bar{\eta}(y, \bar{t})]^{\mathrm{T}}$. The evolution equations for $\bar{v}$ and $\bar{\eta}$ can be put into a vector form similar to (8). The new O–S, Sq, and coupling operators are

$$\bar{\mathscr{L}}_{\mathrm{os}} = -(\mathrm{D}^2 - k^2)^{-1}[\alpha R \mathrm{D}^2 U - \alpha R U(\mathrm{D}^2 - k^2) - \mathrm{i}(\mathrm{D}^2 - k^2)^2], \tag{59}$$

$$\bar{\mathscr{L}}_{\mathrm{sq}} = \alpha R U + \mathrm{i}(\mathrm{D}^2 - k^2), \tag{60}$$

$$\bar{\mathscr{L}}_{\mathrm{c}} = \mathrm{D} U. \tag{61}$$

The advantage of the scaling is that the operators $\bar{\mathscr{L}}_{\mathrm{os}}$ and $\bar{\mathscr{L}}_{\mathrm{sq}}$ depend on only two parameters: $k^2 = \alpha^2 + \beta^2$ and αR. The energy $E(\bar{t})$ of the perturbation $[\bar{v} \, \bar{\eta}]^{\mathrm{T}}$ in the new variables is given by

$$E(\bar{t}) = E_v(\bar{t}) + \beta^2 R^2 E_\eta(\bar{t}) = \int_{-1}^{1} (|\mathrm{D}\bar{v}|^2 + k^2 |\bar{v}|^2) \, \mathrm{d}y + \beta^2 R^2 \int_{1}^{1} |\bar{\eta}|^2 \, \mathrm{d}y. \tag{62}$$

Here, E_v and $\beta^2 R^2 E_\eta$ are the energies in the velocity and normal vorticity, respectively.

The advantage of the new formulation is not clear at this point because of the reappearance of a third parameter, βR, in (62). To motivate the scaling let us consider growth for Poiseuille flow with $\alpha = 0$ and $\beta = O(1)$.

We investigate the growth by examining the effects of the operators $\bar{\mathscr{L}}_{\mathrm{os}}$ and $\bar{\mathscr{L}}_{\mathrm{sq}}$. For $\alpha = 0$, these operators are normal and have spectra lying in the lower half-plane for all k.

The evolution of the velocity is governed solely by $\bar{\mathscr{L}}_{\mathrm{os}}$; we formally have $\bar{v}(y, \bar{t}) = \exp(-\mathrm{i}\bar{\mathscr{L}}_{\mathrm{os}} \bar{t}) \bar{v}(y, 0)$. Since $\bar{\mathscr{L}}_{\mathrm{os}}$ is normal and its spectrum lies in the lower half-plane, the Hille–Yosida theorem implies that $E_v(\bar{t}) \leqslant E_v(0)$ for all $\bar{t} \geqslant 0$.
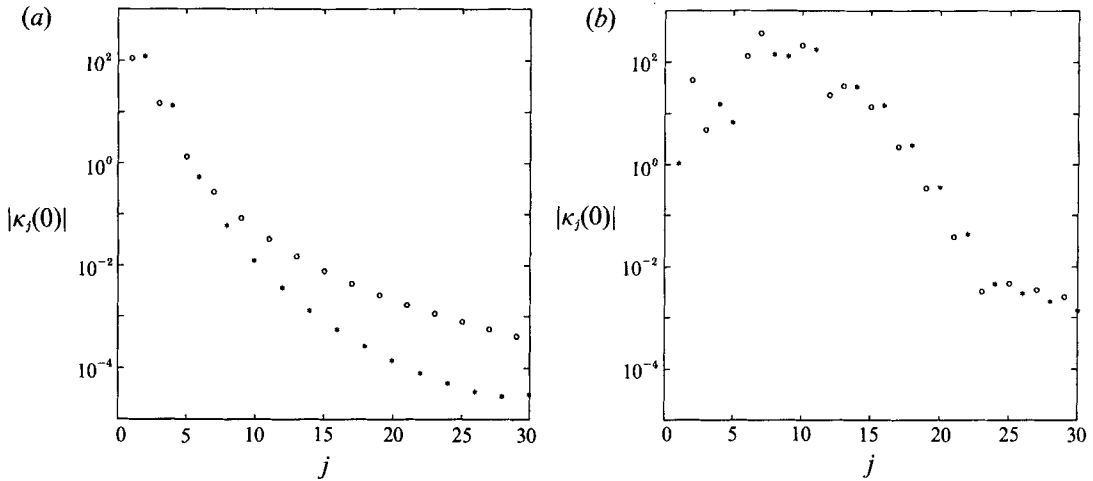
FIGURE 17. (*a, b*) Magnitude of the expansion coefficients of the initial condition that achieves the maximum growth for $R = 1000$ and $\beta = 1.98$. We have $\alpha = 0$ in (*a*) and $\alpha = 1$ in (*b*). $\bigcirc$, O–S modes; *, the Sq modes.

Now, if the initial velocity $\bar{v}$ is zero, then the velocity will remain zero for all time. The normal vorticity is governed by $\mathscr{L}_{sq}$ in this case: $\bar{\eta}(y, \bar{t}) = \exp(-i\mathscr{L}_{sq}\bar{t})\bar{\eta}(y, 0)$. Since $\mathscr{L}_{sq}$ is normal and its eigenvalues lie in the lower half-plane, $E_\eta(\bar{t}) \leqslant E_\eta(0)$ for all $\bar{t} \geqslant 0$. This last result implies that the total energy satisfies $E(\bar{t}) \leqslant E(0)$ if the initial velocity is zero.

These last arguments show that to achieve a large energy growth the initial perturbation $[\bar{v}(y, 0)\ \bar{\eta}(y, 0)]^{\mathrm{T}}$ should be chosen so that most of the initial energy is in the velocity:

$$E_v(0) \gg \beta^2 R^2 E_\eta(0). \tag{63}$$

Let $\bar{t}^{\mathrm{max}}$ denote the time at which the energy of the perturbation has increased by a factor $G^{\mathrm{max}}(0, \beta, R)$. Since $E_v(\bar{t})$, the energy in the velocity, does not grow, it follows that the perturbation that experiences the maximal energy growth satisfies

$$\beta^2 R^2 E_\eta(\bar{t}) \gg E_v(\bar{t}) \quad (\bar{t} \approx \bar{t}^{\mathrm{max}}). \tag{64}$$

This last inequality and the definition of the growth function imply

$$G^{\mathrm{max}}(0, \beta, R) = \sup_{\substack{\bar{v}(y, 0) \neq 0 \\ \bar{t} \geqslant 0}} \frac{E_v(\bar{t}) + \beta^2 R^2 E_\eta(\bar{t})}{E_v(0) + \beta^2 R^2 E_\eta(0)} \tag{65}$$

$$\approx \beta^2 R^2 \sup_{\substack{\bar{v}(y, 0) \neq 0 \\ \bar{t} \geqslant 0}} \frac{E_\eta(\bar{t})}{E_v(0)}. \tag{66}$$

The energies E_v and E_η depend on $\bar{v}$ and $\bar{\eta}$, which in turn only depend on k (since $\alpha = 0$). Hence, the optimization problem in (66) depends only on the parameter $k = \beta$, and we have

$$G^{\mathrm{max}}(0, \beta, R) \approx \beta^2 R^2 H_1(\beta) = R^2 \tilde{H}_1(\beta), \tag{67}$$

for some function $\tilde{H}_1$. (It is convenient to introduce the function $\tilde{H}_1$ because it does not have a singularity at $\beta = 0$.) This scaling relation holds for both Couette and Poiseuille flows and becomes more accurate as R increases.
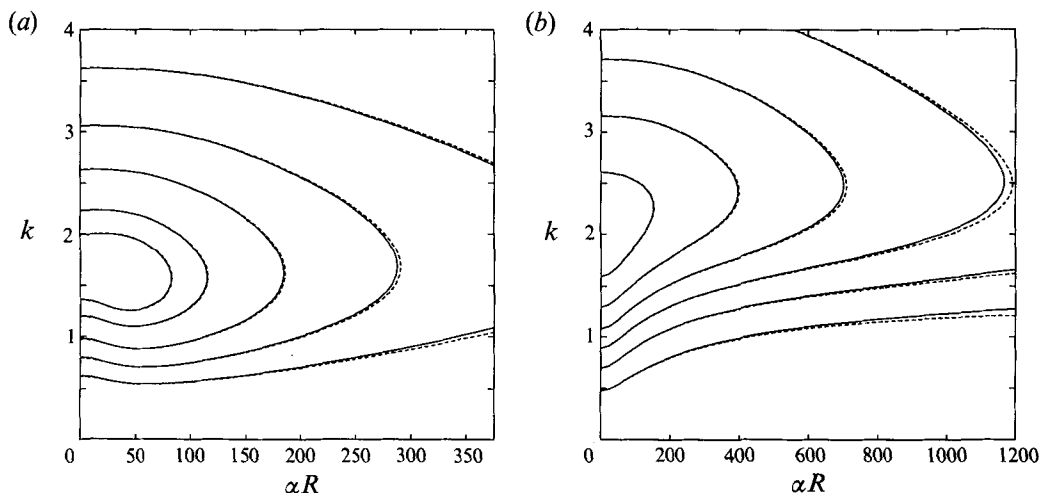
FIGURE 18. (*a, b*) Contours of $k^2 G^{\max}(\alpha, \beta, R)/(\beta^2 R^2)$. For Couette flow (*a*), the contours from outer to inner correspond to 0.4, 0.6, 0.8, 1.0, 1.1 ($\times 10^{-3}$). $---$, $R = 500$; $\underline{\qquad}$, $R = 1000$. For Poiseuille flow (*b*), the contours from outer to inner correspond to 0.3, 0.6, 0.9, 1.2, 1.5, 1.8 ($\times 10^{-4}$). $---$, $R = 1500$; $\underline{\qquad}$, $R = 3000$.

A scaling relation similar to (67) is valid for small αR. To show this we must verify that the initial perturbation achieving a maximum possible energy growth satisfies (63) and (64). For $\alpha \neq 0$, the operators $\mathscr{L}_{\mathrm{os}}$ and $\mathscr{L}_{\mathrm{sq}}$ are non-normal, so the arguments leading to (63) and (64) must be modified.

Now, though $\mathscr{L}_{\mathrm{sq}}$ is non-normal, its numerical range lies in the lower half-plane for $\alpha \geq 0$ (RSH). Hence, by the Hille–Yosida theorem, $E_\eta(\bar{t}) \leqslant E_\eta(0)$ and $E(\bar{t}) \leqslant E(0)$ for all $\bar{t} \geqslant 0$ if the initial velocity is zero. It follows that the initial perturbation must satisfy (63) to achieve the maximum possible energy growth.

The numerical range of $\mathscr{L}_{\mathrm{os}}$ need not lie in the lower half-plane. Hence $E_v(\bar{t})$ may grow, and as we have seen in the last section, there can be significant energy growth for two-dimensional perturbations. However, this growth is much less than the growth for three-dimensional perturbations (≈ 11 compared to ≈ 196 for $R = 1000$, for example). In general, if $G^{\max}(\alpha, \beta, R)$ is large, then the main contribution is due to the energy in the vorticity and (64) must be satisfied.

These arguments imply that (66) holds. In this case, the optimization problem depends on k and αR. Hence, if the three-dimensional growth is 'large', we have

$$G^{\max}(\alpha, \beta, R) \approx \frac{\beta^2 R^2}{k^2} \tilde{H}_2(k, \alpha R) \tag{68}$$

for some function $\tilde{H}_2$. The k^2 term in the numerator ensures that $\tilde{H}_2$ is non-singular as $k \to 0$. Again, (68) becomes more accurate as R increases.

Figure 18 verifies (68) by plotting the level curves of $k^2 G^{\max}(\alpha, \beta, R)/(\beta^2 R^2)$ for Couette and Poiseuille flows in the $(\alpha R, k)$-plane. Comparing results for the two Reynolds numbers, we see that the scaling relation becomes more accurate as $\alpha R \to 0$.

For Poiseuille flow, $S(R) = \sup_{\alpha, \beta} G^{\max}(\alpha, \beta, R)$ is achieved for a point on the β-axis for $R < R_c$, as we saw in the previous subsection. Hence, we can use the scaling relation (67). It follows that S scales like R^2. We find that the maximum of $\tilde{H}_1$ is achieved at $\beta \approx 2.04$ and that

$$S(R) \approx 1.96 \times 10^{-4} R^2 \tag{69}$$

for large subcritical R. This growth is achieved at $t \approx 0.076R$.

For Couette flow, the maximum growth in the (α, β)-plane is achieved near the β-axis. The scaling relation (68) and the results in figure 18(a) imply that the largest growth in the (α, β)-plane is achieved for $k \approx C_1$ and $\alpha R \approx C_2$, where C_1 and C_2 are constants. If we substitute these constants into (68) and use the fact that $\beta^2 = k^2 - \alpha^2$, we find that

$$\frac{\beta^2 R^2}{k^2} \tilde{H}_2(k, \alpha R) = R^2 \left(1 - \frac{C_2^2}{C_1^2 R^2} \right) \tilde{H}_2(C_1, C_2). \tag{70}$$

Hence, the growth scales like R^2 as $R \to \infty$. This result verifies the results in Butler & Farrell (1992), where it is shown that

$$S(R) \approx 1.18 \times 10^{-3} R^2 \tag{71}$$

and that the maximum growth occurs at $t \approx 0.117R$. We find that $C_1 \approx 1.6, C_2 \approx 35$.

8. Discussion

In this paper we have investigated energy growth for small two- and three-dimensional perturbations to Couette and Poiseuille flows.

There is more to the linear operator $\mathcal{L}$, which governs the evolution of small perturbations to channel flows, then its eigenvalues. The reason is that $\mathcal{L}$ is non-normal; it has non-orthogonal eigenfunctions. In such cases it is often more appropriate to analyse the numerical range and the ϵ-pseudospectra to understand the operator behaviour. A fundamental implication of the non-normality is that there can be substantial transient growth in the energy of small perturbations even if the Reynolds number is less than the critical value. This growth occurs in the absence of nonlinearities.

Our main focus has been to calculate the growth function $G(\alpha, B, R, t)$, which gives the maximum potential growth for small perturbations for the wavenumber combination (α, β), Reynolds number R, and time t, and the maximum growth $G^{\max}(\alpha, \beta, R)$, which gives the maximum growth for all time. The maximum growth has three types of behaviour. First, if $\mathcal{L}$ has an eigenvalue in the upper half-plane, the flow is linearly unstable, then $G^{\max} = \infty$. Secondly, if the numerical range of $\mathcal{L}$ lies in the lower half-plane, then $G^{\max}(\alpha, \beta, R) = 1$, and there is no growth. We show that there is a function $R_1(\alpha, \beta)$ such that there is no growth if $R \leqslant R_1(\alpha, \beta)$. Finally, if $R > R_1(\alpha, \beta)$ and the flow is linearly stable, then $1 < G^{\max}(\alpha, \beta, R) < \infty$, and there is transient growth. Our numerical procedure for computing transient growth is similar to that used by Butler & Farrell (1992).

We find that there is transient growth if $k^2 = \alpha^2 + \beta^2$ satisfies $k_1(R) \leqslant k^2 \leqslant k_2(R)$, where $k_1 \to 0$ and $k_2 \to \infty$ as $R \to \infty$. For fixed Reynolds number, the maximum growth $G^{\max}(\alpha, \beta, R)$ is largest for $\alpha \ll 1$ and $\beta = O(1)$. By generalizing a scaling argument introduced by Gustavsson (1991), we show that for moderate αR, $G^{\max}(\alpha, \beta, R)$ effectively depends on the two parameters $k^2 = \alpha^2 + \beta^2$ and αR. Using this relation, we show that $\sup_{\alpha, \beta} G^{\max}(\alpha, \beta, R) = O(R^2)$ at subcritical Reynolds numbers. Finally, we show numerically that $G^{\max}(\alpha, \beta, R)$ is smooth at points in the parameter space where the Orr–Sommerfeld operator has a degenerate eigenvalue or where an Orr–Sommerfeld and a Squire eigenvalue coincide.

The function $G(\alpha, \beta, R, t)$ for fixed time, which is plotted in figure 16, can be used to analyse growth for localized disturbances. The Fourier transform in the horizontal directions of such a disturbance gives a corresponding distribution in a region in

wavenumber space. The growth in physical space can be maximized if the growth is maximized for each (α, β) at a particular time. In previous work, Henningson (1991) found transient growth by choosing an arbitrary localized disturbance. Using the singular value decomposition, it is straightforward to determine the optimal form of $\hat{v}(y, 0)$ and $\hat{\eta}(y, 0)$ for each wavenumber combination, so that the total energy growth is larger.

Although the global optimal growth is achieved at or near the β-axis it is also important to examine growth for non-zero α for several reasons. First, away from the β-axis the growth function $G(\alpha, \beta, R, t)$ is maximized for relatively small t. In the simulations of transition of localized disturbances in plane Poiseuille flow, it was found that transition usually occurred significantly earlier than the time for the global optimum (Henningson, Lundbladh & Johansson 1993). Secondly, nonlinear interactions are much richer when oblique waves are present than when waves with $\alpha = 0$ only exist. If a disturbance consists only of waves with $\alpha = 0$, then no wavenumber with a non-zero α can be excited.

In our analysis of conditions for no growth for Poiseuille and Couette flows, we find that R_g, the largest Reynolds number below which there is no growth for perturbations of arbitrary amplitude, is the same as that obtained by analysing the linear operator $\mathcal{L}$. This occurs because the nonlinear terms drop out of the Reynolds–Orr equation. This connection has interesting implications. First, it implies that there can be no growth of perturbations of arbitrary amplitude unless there is a linear growth mechanism. Secondly, it explains the difference between R_c and R_g; the difference exists because the governing linear operator $\mathcal{L}$ is non-normal. (The converse need not be true; if the linear operator is non-normal then it is possible for R_c and R_g to be the same.) Other classes of flows for which R_c and R_g differ include pipe flows (Joseph & Carmi 1969) and a convective flow with surface tension (Davis 1969). On the other hand, $R_g \equiv R_c$ for the Bénard convection problem, involving the stability of a motionless fluid between two heated plates (Joseph 1965). It can be shown that the governing linear operator is normal.

The recent numerical simulations of Henningson *et al.* (1993) and Schmid & Henningson (1992) demonstrate the importance of transient growth for subcritical transition; it is shown that linear mechanism plays an important role for growth of finite-amplitude disturbances. The main conclusion is that as soon as nonlinear effects transfer energy into waves that experience rapid transient growth, the linear growth mechanism is activated. That energy is subsequently used to supply other wavenumbers with energy, rapidly moving the flow to a turbulent state. This mechanism results in a bypass of the traditional secondary instability scenario.

The connection between linear stability analysis and stability for the full nonlinear problem has been studied previously. For example, Galdi & Straughan (1985) consider evolution equations similar to the Navier–Stokes equations. They prove that if the governing linear operator is self-adjoint and the nonlinear terms satisfy certain conditions, then linear stability implies that there is no energy growth for perturbations of arbitrary amplitude. This result can be applied to the Bénard problem. In general, one must check that the technical conditions are satisfied on a case by case basis. We have not attempted to prove general stability results here. However, we would like to stress that there is always the potential for subcritical transition if the governing linear operator is non-normal.

REFERENCES

BENNEY, D. J. & GUSTAVSSON, L. H. 1981 A new mechanism for linear and nonlinear hydrodynamic instability. *Stud. Appl. Maths* **64**, 185–209.

BUSSE, F. H. 1969 Bounds on the transport of mass and momentum by turbulent flow between parallel plates. *Z. angew. Math. Phys.* **20**, 1–14.

BUTLER, K. M. & FARRELL, B. F. 1992 Three-dimensional optimal perturbations in viscous shear flows. *Phys. Fluids* A **4**, 1637–1650.

CANUTO, C., HUSSAINI, M. Y., QUARTERONI, A. & ZANG, T. A. 1988 *Spectral Methods in Fluid Dynamics*. Springer.

DAVIS, S. H. 1969 Buoyancy-surface tension instability by the method of energy. *J. Fluid Mech.* **39**, 347–359.

DIPRIMA, R. C. & HABETLER, G. J. 1969 A completeness theorem for non-selfadjoint eigenvalue problems in hydrodynamic stability. *Arch. Rat. Mech. Anal.* **34**, 218–227.

DRAZIN, P. G. & REID, W. H. 1981 *Hydrodynamic Stability*. Cambridge University Press.

FARRELL, B. F. 1988 Optimal excitation of perturbations in viscous shear flow. *Phys. Fluids* **31**, 2093–2102.

GALDI, G. P. & STRAUGHAN, B. 1985 Exchange of stabilities, symmetry, and nonlinear stability. *Arch. Rat. Mech. Anal.* **89**, 211–228.

GUSTAVSSON, L. H. 1986 Excitation of direct resonances in plane Poiseuille flow. *Stud. Appl. Maths* **75**, 227–248.

GUSTAVSSON, L. H. 1991 Energy growth of three-dimensional disturbances in plane Poiseuille flow. *J. Fluid Mech.* **224**, 241–260.

GUSTAVSSON, L. H. & HULTGREN, L. S. 1980 A resonance mechanism in plane Couette flow. *J. Fluid Mech.* **98**, 149–159.

HENNINGSON, D. S. 1988 The inviscid initial value problem for a piecewise linear mean flow. *Stud. Appl. Maths* **78**, 31–56.

HENNINGSON, D. S. 1991 An eigenfunction expansion of localized disturbances. In *Advances in Turbulence 3* (ed. A. V. Johansson & P. H. Alfredsson). Springer.

HENNINGSON, D. S., LUNDBLADH, A. & JOHANSSON, A. V. 1993 A mechanism for bypass transition from localized disturbances in wall bounded shear flows. *J. Fluid Mech.* **250**, 169–207.

HENNINGSON, D. S. & SCHMID, P. J. 1992 Vector eigenfunction expansions for plane channel flows. *Stud. Appl. Maths* **87**, 15–45.

HERBERT, T. 1977 *Die Neutrale Fläche der Ebenen Poiseuille-Strömung*. Habilitationsschrift, Universität Stuttgart.

HERBERT, T. 1988 Secondary instability of boundary layers. *Ann. Rev. Fluid Mech.* **20**, 487–526.

HERRON, I. H. 1980 A completeness observation on the stability equations for stratified viscous shear flows. *Phys. Fluids* **23**, 836–837.

HERRON, I. H. 1991 Observations on the role of the vorticity in the stability of wall bounded flows. *Stud. Appl. Maths* **85**, 269–286.

JOSEPH, D. D. 1965 On the stability of the Boussinesq equations. *Arch. Rat. Mech. Anal.* **20**, 59–71.

JOSEPH, D. D. 1966 Nonlinear stability of the Boussinesq equations by the method of energy. *Arch. Rat. Mech. Anal.* **22**, 163–184.

JOSEPH, D. D. 1969 Eigenvalue bounds for the Orr–Sommerfeld equation. Part 2. *J. Fluid Mech.* **36**, 721–734.

JOSEPH, D. D. 1976 *Stability of Fluid Motions I*. Springer.

JOSEPH, D. D. & CARMI, S. 1969 Stability of Poiseuille flow in pipes, annuli and channels. *Q. Appl. Maths* **26**, 575–599.

KATO, T. 1976 *Perturbation Theory for Linear Operators*. Springer.

LANDAHL, M. T. 1975 Wave breakdown and turbulence. *SIAM J. Appl. Maths* **28**, 733–756.

LANDAHL, M. T. 1980 A note on an algebraic instability of inviscid parallel shear flows. *J. Fluid Mech.* **98**, 243–251.

LUNDBLADH, A. & JOHANSSON, A. V. 1991 Direct simulation of turbulent spots in plane Couette flow. *J. Fluid Mech.* **229**, 499–516.

ORR, W. M'F. 1907 The stability or instability of the steady motions of a perfect liquid and of a viscous liquid. Part II: A viscous liquid. *Proc. R. Irish Acad.* A **27**, 69–138.

ORSZAG, S. A. 1971 Accurate solution of the Orr–Sommerfeld equation. *J. Fluid Mech.* **50**, 689–703.

PATEL, V. C. & HEAD, M. R. 1969 Some observations on skin friction and velocity profiles in fully developed pipe and channel flows. *J. Fluid Mech.* **38**, 181–201.

PAZY, A. 1983 *Semigroups of Linear Operators and Applications to Partial Differential Equations.* Springer.

REDDY, S. C., SCHMID, P. J. & HENNINGSON, D. S. 1993 Pseudospectra of the Orr–Sommerfeld operator. *SIAM J. Appl. Maths* **53**, 15–47.

SCHMID, P. J. & HENNINGSON, D. S. 1992 A new mechanism for rapid transition involving a pair of oblique waves. *Phys. Fluids* A **4**, 1986–1989.

SHANTINI, R. 1989 Degeneracies of the temporal Orr–Sommerfeld eigenmodes in plane Poiseuille flow. *J. Fluid Mech.* **201**, 13–34.

SYNGE, J. L. 1938 Hydrodynamic stability. *Semicentenn. Publ. Amer. Math. Soc.* **2**, 227–269.

TILLMARK, N. & ALFREDSSON, H. 1992 Experiments on transition in plane Couette flow. *J. Fluid Mech.* **235**, 89–102.

TREFETHEN, L. N. 1992 Pseudospectra of matrices. In *Numerical Analysis 1991* (ed. D. F. Griffiths & G. A. Watson). Longman.

TREFETHEN, L. N., TREFETHEN, A. E., REDDY, S. C. & DRISCOLL, T. A. 1992 A new direction in hydrodynamic stability: beyond eigenvalues. *Tech. Rep. CTC* 92TR115, Cornell Theory Center, Cornell University.